Basin Research

Basin Research (2011) 23, 403–422, doi: 10.1111/j.1365-2117.2010.00495.x

Intraplate subsidence and basin filling adjacent to an oceanic arc–continent collision: a case from the southern Caribbean-South America plate margin

Germán Bayona*,†, Camilo Montes,†,‡ Agustín Cardona,†,‡ Carlos Jaramillo,† Germán Ojeda,§ Victor Valencia¶ and Carolina Ayala-Calvo‡

*Corporación Geológica ARES, Bogotá, Colombia, Calle 44A N. 53-96, USA
†Smithsonian Tropical Research Institute, Unit 0948. APO AA 34002-0948, USA
‡Corporación Geológica ARES, Bogotá, Colombia, Calle 44A N. 53-96
§ECOPETROL S.A., Bogotá, Colombia
¶School of Earth and Environmental Sciences, Washington State University, Pullman, WA 99164-2812 85721, USA

ABSTRACT

The upper Campanian–Lower Eocene synorogenic sedimentary wedge of the Ranchería Basin was deposited in an intraplate basin resting on a tilted continental crustal block that was deformed by collision and subsequent subduction of the Caribbean Plate. Upper Cretaceous–Lower Eocene strata rest unconformably upon Jurassic igneous rocks of the Santa Marta Massif, with no major thrust faults separating the Santa Marta Massif from the Ranchería Basin. The upper Campanian–Lower Eocene succession includes, from base to top: foraminifera-rich calcareous mudstone, mixed carbonate–siliciclastic strata and mudstone, coal and immature fluvial sandstone beds. Diachronous collision and eastward tilting of the plate margin (Santa Marta Massif and Central Cordillera) favoured the generation of accommodation space in a continuous intraplate basin (Ranchería, Cesar and western Maracaibo) during the Maastrichtian to Late Palaeocene. Terrigenous detritus from the distal colliding margin filled the western segments of the continuous intraplate basin (Ranchería and Cesar Basins); in the Late Paleocene, continental depositional systems migrated eastwards as far as the western Maracaibo Basin. In Early Eocene time, reactivation of former extensional structures fragmented the intraplate basin into the Ranchería-Cesar Basins to the west, and the western Maracaibo Basin and Palmar High to the East. This scenario of continent–oceanic arc collision, crustal-scale tilting, intraplate basin generation and fault reactivation may apply for Upper Cretaceous–Palaeogene syntectonic basins in western Colombia and Ecuador, and should be considered in other settings where arc–continent collision is followed by subduction.

INTRODUCTION

The relationships among growth of fault systems, stratal geometry and stacking patterns in syntectonic basins have been well documented for rift basins (McKenzie, 1978; Lister *et al.*, 1986; Gawthorpe & Leeder, 2000) and foreland basins (Beaumont *et al.*, 1988; Jordan & Flemings, 1991; DeCelles & Giles, 1996; Sinclair, 1997). In contractional tectonic settings, such as the central and northern Andes, subduction and terrane accretion control the generation and filling of forearc basins (e.g. Cediel *et al.*, 2003; Fildani *et al.*, 2008, Jaillard *et al.*, 2009), whereas the thickening of continental crust (i.e. the orogenic belt) controls the generation and filling of foreland basins (see Hoorn & Wesselingh, 2010 for a review of the Amazonas foreland basin). In contrast, the mechanism of formation and filling of intraplate basins resting on continental crust not bounded by major faults is less well understood (e.g. Pindell *et al.*, 2005). The northwestern South America margin contains good examples of such basins (Fig. 1), where the northeastward drift of the thick and buoyant Caribbean Plateau and its frontal magmatic arc (Burke, 1988; Pindell *et al.*, 1998; Acton *et al.*, 2000) drove oblique collision of oceanic-cored terranes with the South American plate. This collision generated continental-arc magmatism along the continental margin (Cardona *et al.*, 2010; in press) (Fig. 1, inset) and intraplate basins, which were completely filled with synorogenic continental deposits in the Late Palaeocene (Pindell *et al.*, 1998; Villamil, 1999; Gómez *et al.*, 2005; Bayona *et al.*, 2008).

This paper documents basin generation, subsidence and subsequent rapid filling with continental sediments of two intraplate basins and links the evolution of these basins to collisional and magmatic processes along the

Correspondence: Germán Bayona, Corporación Geológica ARES, Bogotá, Colombia, Calle 44A N. 53-96 and Smithsonian Tropical Research Institute, Unit 0948, APO AA 34002-0948, USA. E-mail: gbayona@cgares.org

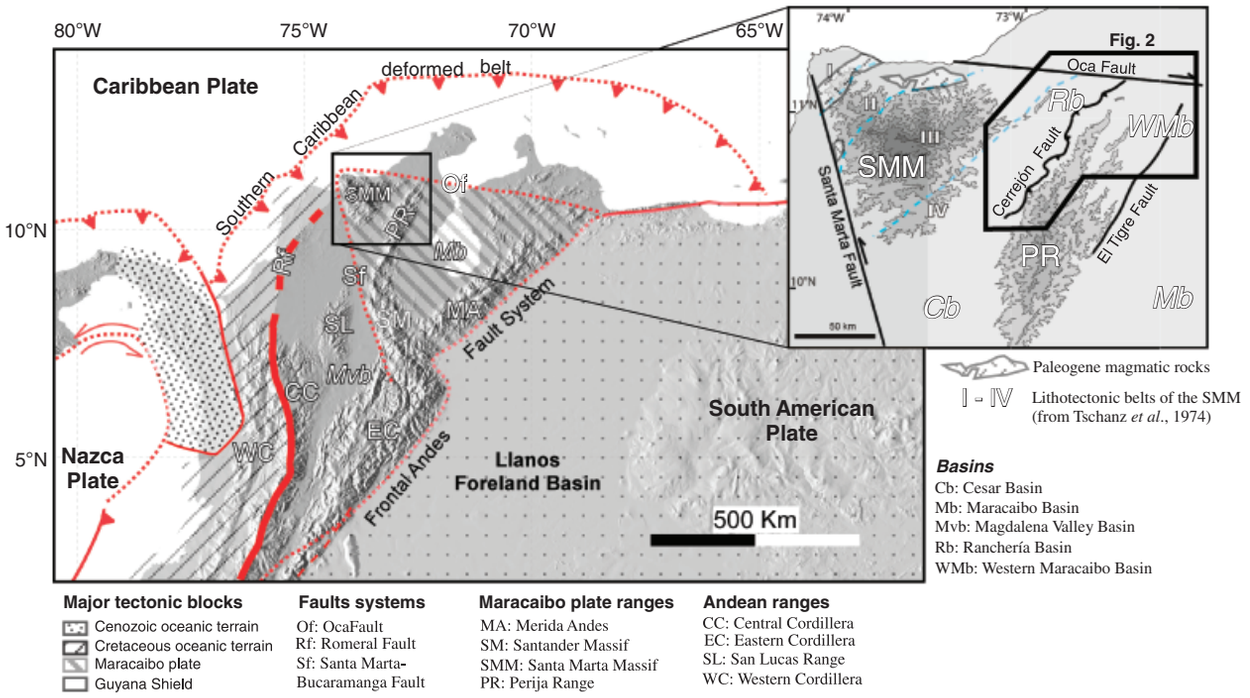

Fig. 1. Regional tectonic setting of the northern Andes and southern Caribbean Plate showing the location of Ranchería, Cesar, western Maracaibo and northern Middle Magdalena Basins. Inset (upper right) shows location of Cesar and Ranchería Basins between the Santa Marta Massif and the Perijá Range. Lithotectonic belts of the Santa Marta Massif, as defined by Tschanz *et al.* (1974), are shown with Roman numerals (I–IV); Palaeogene magmatic rocks intrude belts I, II and III. Shades of grey represent elevation (contour intervals in kilometres).

northwestern South America margin. We studied the Ranchería Basin, which is bounded by the Santa Marta Massif on the northwest and the Perijá Range on the southeast and the westernmost Maracaibo Basin, whose strata outcrop in the Manuelote Syncline located in the eastern foothills of the Perijá Range (Fig. 2). The integration of these analyses and of similar data reported in the Cesar Basin (Ayala-Calvo *et al.*, 2009) and the northern Magdalena Basin (Gómez *et al.*, 2005) allows us to understand the regional response of these intraplate basins to the Caribbean magmatic arc collision and subduction history.

Our results contribute to the understanding of uplift processes and generation of intraplate syntectonic basins that are not controlled by major faults along the western margin of the northwestern South America plate. Similar tectonic settings can be found in other areas where oceanic plates, oceanic magmatic arcs or continental crustal blocks have a complex collision and subduction history, such as intraplate basins in Ecuador (Jaillard *et al.*, 2002, 2008; Toro-Alava & Jaillard, 2005) and northern Papua New Guinea (Abbott *et al.*, 1994).

TECTONIC FRAMEWORK OF THE NORTHERN ANDES–CARIBBEAN PLATE BOUNDARY

Regional tectonic setting

The Cretaceous–Cenozoic interactions between the Caribbean Plate and continental blocks of the South American plate (Pindell *et al.*, 1998, 2005) produce the present complex structural configuration that includes, from west to east, the Santa Marta Massif, the Ranchería and Cesar Basins, the Perijá Range and the western Maracaibo Basin (Figs 1 and 2). North of the east-striking dextral Oca Fault system, thick Neogene deposits separate isolated massifs disrupted by dextral transtensional faults (Alvarez, 1971).

The Santa Marta Massif comprises four lithotectonic belts (Tschanz *et al.*, 1974) (Fig. 1, inset), which are described from the northwest to the southeast. Belt I consists of orthogneisses and a low-grade metamorphosed volcanic-sedimentary belt (arc basin was active by ca. 82 Ma, according to U/Pb detrital zircon ages from the sedimentary protolith, Cardona *et al.*, 2010) affected by latest Cretaceous metamorphism (MacDonald *et al.*, 1971; Tschanz *et al.*, 1974; Cardona *et al.*, 2010). Belt II includes amphibolite facies rocks with a 530 Ma maximum protolith age and two-mica schist with associated Permian granitoids (Cardona-Molina *et al.*, 2006; Cardona *et al.*, 2010). Belt III consists of granulite facies and associated metamorphosed anorthosites with a 1.25-Ga protolith (Cordani *et al.*, 2005) recording the Grenvillian orogeny (ca 1.16–0.9 Ga, Restrepo-Pace *et al.*, 1997; Cordani *et al.*, 2005); isolated upper Palaeozoic sedimentary rocks are reported in this belt (Tschanz *et al.*, 1974). Palaeocene and lower Eocene granitoids (50–65 Ma) intrude rocks of belts I–III (Tschanz *et al.*, 1974; Cardona *et al.*, in press; Fig. 1, inset), whereas granitoids of Jurassic age extensively intrude belt III. Belt IV consists of weakly deformed Triassic–Jurassic volcaniclastic and plutonic rocks unconformably overlain by the Upper Cretaceous–Lower Eocene sedimentary succession (Montes *et al.*, 2010) (Figs 2 and 3); faults and folds

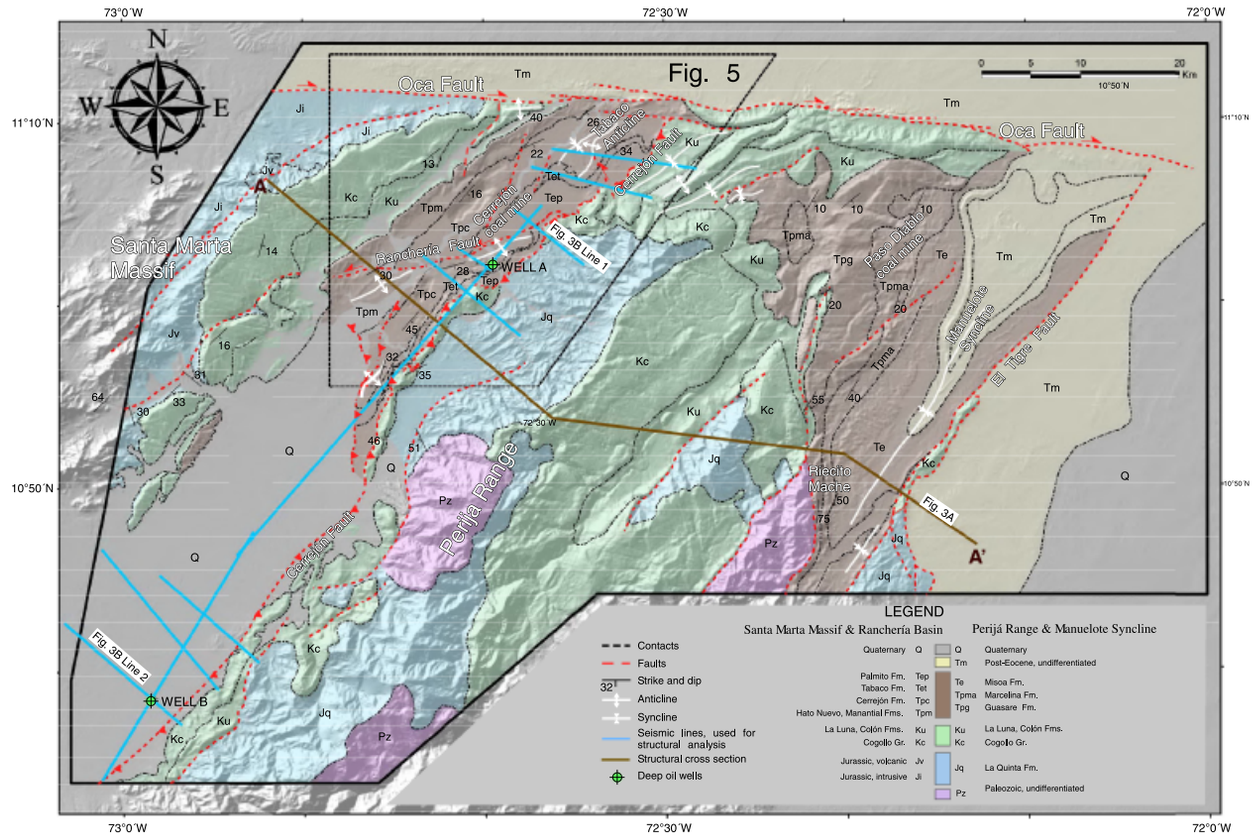

Fig. 2. Geologic map of the northern Ranchería Basin and the Perijá Range (compiled from Tschanz *et al.*, 1974; Bellizzia *et al.*, 1976; Montes *et al.*, 2010) showing the location of study areas (Cerrejón coal mine, Paso Diablo coal mine, Riecito Mache), deep seismic lines for structural control and deep oil wells A and B.

only locally disrupt the fourth belt. A similar homocline structure has been documented farther south in the western flank of the northern Magdalena Valley (Pindell & Kennan, 2009).

Upper Cretaceous–Palaeocene plutonic rocks from the Santa Marta Massif document the growth of a Caribbean magmatic arc during the Late Cretaceous, followed by collision of this Caribbean arc with the continent by the early Maastrichtian (~70 Ma). As result of the collision, an eastward-dipping subduction of the Caribbean Plate formed from the outside the accreted arc (Cardona *et al.*, in press). This subduction produced continental magmatism during Palaeocene–Early Eocene time (Cardona *et al.*, in press) (Fig. 1, inset).

The Perijá Range separates the Cesar-Ranchería Basin to the west and the western Maracaibo Basin to the east (Figs 1 and 2). Mesozoic volcaniclastic and sedimentary rocks dominate the northern Perijá Range, with a minor proportion of sedimentary Palaeozoic rocks (Miller, 1962; Bellizzia *et al.*, 1976; Dasch, 1982; Kellogg, 1984; Maze, 1984; Forero, 1990; Ujueta & Llinás, 1992) (Fig. 2). The northern Perijá Range is bounded to the west by the northwest-verging Cerrejón Fault system (Figs 2 and 3) and to the east by the El Tigre Fault. The latter fault has been interpreted as: (1) an Oligocene northwest-verging thrust fault (Kellogg, 1984); (2) a northwest-dipping strike-slip fault with down-to-the-west (extensional) activity in Jurassic and Palaeocene time, and positive reactivation in Mio-Pliocene time (Miller, 1962; Quijada & Cassani, 1997); (3) an Eocene strike-slip fault (Pindell *et al.*, 1998); or (4) a southeast-dipping normal fault inverted in Neogene time (Duerto *et al.*, 2006).

Cretaceous–Lower Eocene tectonostratigraphic units

Sedimentary basins to the east of the Central Cordillera, San Lucas Range and Santa Marta Massif have similar tectonic evolution and depositional trends. Lower Cretaceous extensional basins were filled with siliciclastic rocks, and in the Perijá Range the Lower Cretaceous succession is known as the Rio Negro Formation (Miller, 1962; Caceres *et al.*, 1980) (Fig. 4). In the Ranchería-Cesar Basins and western Maracaibo Basin, Aptian-Albian carbonates of the Cogollo Group diachronously covered Triassic–Jurassic plutonic and volcaniclastic rocks (Fig. 4) (Tschanz *et al.*, 1974; Caceres *et al.*, 1980; Quijada & Cassani, 1997). Bituminous limestone, shales and chert of Turonian to Santonian age (La Luna Formation; Caceres *et al.*, 1980; Villamil & Arango, 1998) record deep-water accumulation (outer ramp, Martínez & Hernández, 1992). This deep-water and anoxic deposition continued until middle Campanian time (Fig. 4, Tres Esquinas and Socuy members of the Colón Formation; Martínez & Hernández, 1992). These deep-water

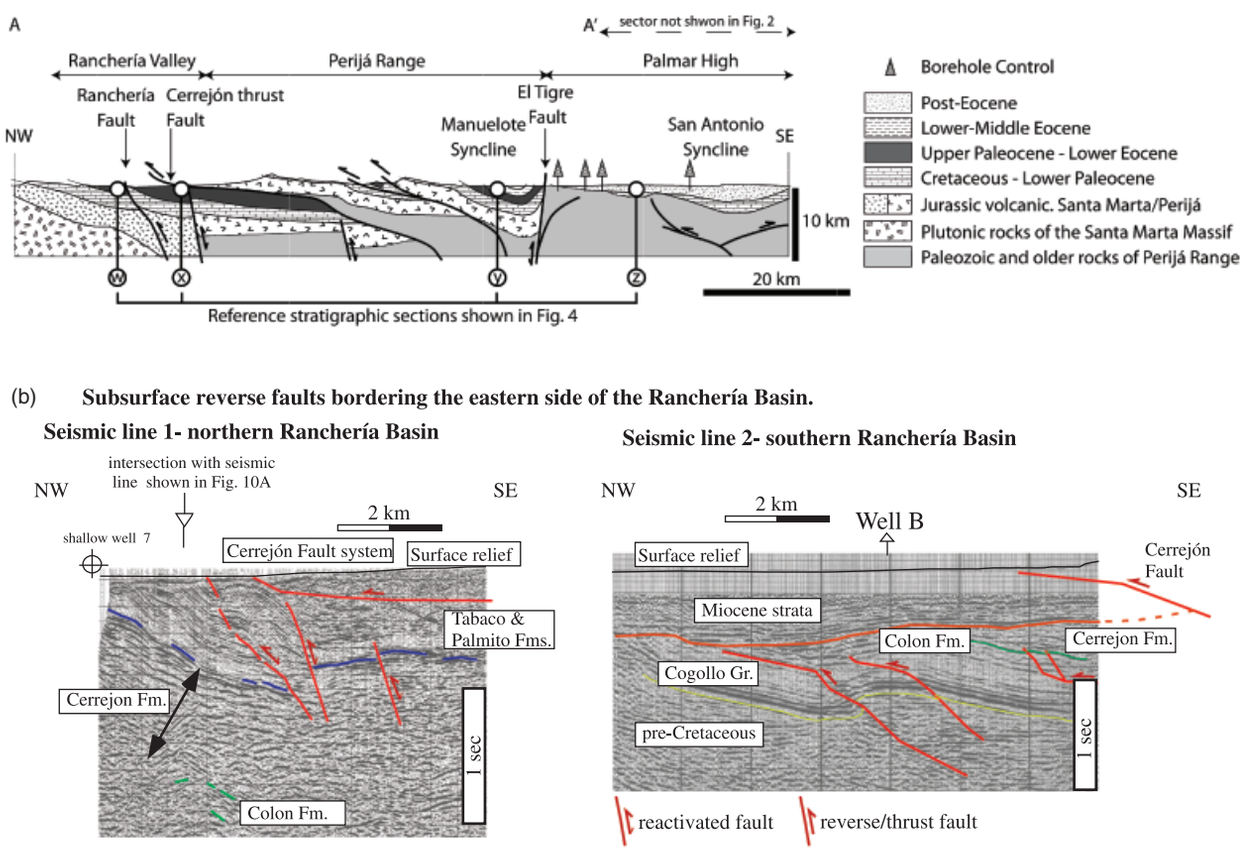

Fig. 3. (A) Regional cross section A–A′ (modified from Kellogg, 1984) shows the depositional contact between Cretaceous and Jurassic rocks of the Santa Marta Massif, the homocline structure of the Ranchería Basin, the low angle southeast-dipping Cerrejón Fault. The high-angle El Tigre Fault limits the Manuelote Syncline from the Palmar High. See also the location of reference stratigraphic sections W, X, Y and Z used for chronostratigraphic correlation in Fig. 4. (B) Interpretation of deep seismic lines showing subsurface high-angle, northwest-verging faults and folds beneath the Cerrejón Fault (seismic line 1) and Miocene strata (seismic line 2).

marine deposits were overlain by shallow-marine to continental sediments of a first-order regressional succession that lasted until the Early Eocene (Villamil, 1999). The upper Campanian–Lower Eocene sedimentary succession, the focus of this study, is described in detail in this paper.

An angular unconformity overlies Lower Eocene (or older) strata in the Ranchería-Cesar Basins and western Maracaibo Basin. In the southern part of the Ranchería Basin, undeformed and undated conglomerate beds overlie Maastrichtian–Paleocene strata; these beds have been assumed to be of Miocene age (Caceres *et al.*, 1981), and they are bounded to the east by the Cerrejón Fault (Fig. 3b, seismic line 2). In the Manuelote Syncline, Upper Eocene strata rest unconformably upon Lower Eocene–Palaeocene strata (Bellizzia *et al.*, 1976). However, East of the Manuelote Syncline and the El Tigre Fault, post-Eocene strata rest in angular unconformity upon Palaeocene to Palaeozoic rocks in a structure named the El Palmar High (Figs 3a and 4; Miller, 1962; Kellogg, 1984; Quijada & Cassani, 1997). Farther to the east in the Maracaibo Lake, Lower Eocene strata unconformably overlie Palaeocene strata and underlie Oligocene and younger strata (Lugo & Mann, 1995; Escalona & Mann, 2006).

METHODS

The intraplate basin generation and filling processes in the Ranchería and western Maracaibo Basins were determined on the basis of geologic mapping, geometry and stacking patterns of upper Campanian–Lower Eocene strata, provenance and subsidence analysis.

The present boundaries of the Ranchería and western Maracaibo Basins and the Perijá Range were defined using geologic mapping and subsurface control of structures. The Upper Cretaceous–Lower Eocene succession in the Ranchería Basin and western Maracaibo Basin were mapped using field data collected from the Cerrejón coal mine (Ranchería Basin, modified from Montes *et al.*, 2010), and from the Paso Diablo coal mine and Riecito Mache in the Manuelote Syncline (western Maracaibo Basin). Mapping of other units was taken from published geologic maps (Tschanz *et al.*, 1974; Bellizzia *et al.*, 1976). The internal geometry of the Ranchería Basin was determined from five northwest-striking seismic lines around well A, three northwest-striking seismic lines around well B and two northeast-striking seismic lines linking wells A and B (Fig. 2). The regional cross section of Kellogg (1984)

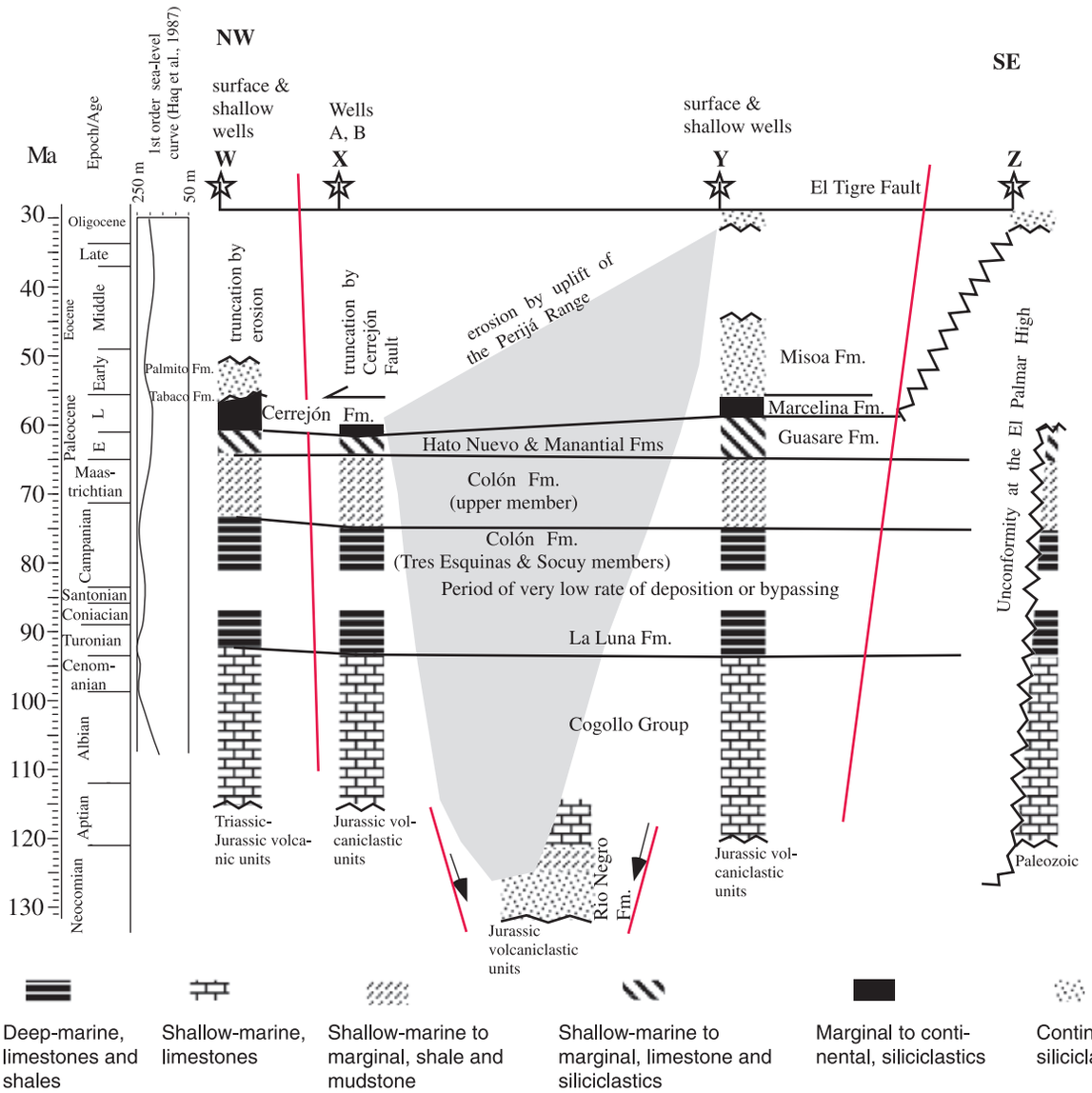

Fig. 4. Upper Neocomian–Middle Eocene chronostratigraphic correlation of reference stratigraphic sections W, X, Y and Z (see Fig. 3 for location). W = western Ranchería Basin (composite stratigraphic section measured to the north of the Ranchería Fault); X = eastern Ranchería Basin (composite stratigraphic section from wells A and B); Y = composite stratigraphic section in the western flank of the Manuelote Syncline; Z = descriptions from wells in the Palmar High (data from Quijada & Cassani, 1997).

was modified using our surface and subsurface observations in the Ranchería Basin.

Lithological descriptions of the Upper Campanian–Lower Eocene succession in the Ranchería Basin were made from: (1) γ-ray profiles and well-cutting descriptions of wells A and B for upper Campanian to Lower Palaeocene units; (2) descriptions of cores from six shallow wells of the Cerrejón coal mine and (3) descriptions of outcrops in the Cerrejón coal mine (Ranchería Basin) for Palaeocene–Lower Eocene units. For the western Maracaibo Basin (western flank of the Manuelote Syncline, Fig. 2), we used: (1) cores from shallow wells, (2) descriptions of outcrops from the Paso Diablo coal mine for Palaeocene–Lower Eocene units, and (3) descriptions of outcrops of the Upper Palaeocene–Lower Eocene succession in Riecito Mache (Fig. 2), which were complemented with descriptions of Lower Eocene strata presented in Pardo (2004). Biostratigraphic reports for wells A and B (Bioss, 1995) were revised and updated using the biozones of Jaramillo *et al.* (in press).

Stacking patterns of deposition of the Palaeocene–Lower Eocene succession were defined by the identification of flooding surfaces. Seismic reflection profiles in little deformed areas and with well control were used to characterize stratigraphic units and flooding surfaces, as well as to identify two-dimensional strata geometry and internal strata truncations. One-dimensional backstripping follows the methods and assumptions specified in Watts & Ryan (1976) and Allen & Allen (1992). The Late Cretaceous–Cenozoic first-order sea level curve of Haq *et al.* (1987) was used for eustasy correction of tectonic subsidence curves.

The provenance analysis integrates petrographic information, U/Pb detrital zircon ages and palaeocurrent indicators reported for the Ranchería, Cesar and western Maracaibo Basins (methods and raw data presented in Appendix S1).

RESULTS

Structure of the Ranchería basin, Northern Perijá range and Manuelote Syncline

The Ranchería Basin is bounded to the west by a low-angle, southeast-dipping homocline formed by the Upper Cretaceous–Lower Eocene sedimentary cover succession resting unconformably upon Jurassic igneous rocks of the Santa Marta Massif (Figs 1 and 2). Strike-slip and reverse faults affect Jurassic rocks of the Santa Marta Massif (Tschanz *et al.*, 1974). The left-lateral Ranchería Fault separates the Palaeocene–Lower Eocene sedimentary succession in the Ranchería Basin into two domains (Fig. 2). The northern domain includes the Tabaco Anticline and minor faults dislocating the homocline, whereas the southern domain includes west-verging reverse faults and folds striking sub-parallel to the Ranchería Fault. Palaeocene stratigraphic units were measured in the northern domain, where deformation is less intense than in the southern domain.

The northwest-verging Cerrejón Fault forms the eastern boundary of the Ranchería Basin (Fig. 3). Detailed mapping of the irregular and curved trace of the fault (Montes *et al.*, 2010) indicates a low-angle dip, as identified by Kellogg (1984). Seismic lines near well A show that the Cerrejón Fault decapitates subsurface high-angle northwest-verging faults and folds (Fig. 3b, seismic line 1). Farther south, near well B, the Cerrejón Fault limits Miocene strata; these little deformed strata overlie in angular unconformity northwest-verging faults and folds involving Lower Palaeocene, Cretaceous and pre-Cretaceous units (Fig. 3b, seismic line 2). These subsurface faults and related folds form the western boundary of the Perijá Range in the subsurface (Fig. 3a). These structural observations, and a maximum thickness of 2.5 km for Palaeocene strata calculated in this study (see next section), were incorporated in Kellogg's (1984) cross-section (Fig. 3a).

The Perijá Range includes a northeast-plunging anticline cored by Jurassic rocks in the hanging wall of the Cerrejón Fault. The frontal limb exposes tight folds, whereas the backlimb forms a shallowly dipping homocline defined by Cretaceous beds, as documented by Kellogg & Bonini (1982). To the north, Upper Cretaceous beds are folded in easterly striking structures.

The El Tigre Fault separates the thick Jurassic–Lower Eocene volcano-sedimentary succession in the Manuelote Syncline from the El Palmar High to the west. The Manuelote Syncline is a northeast-striking and plunging asymmetrical fold whose axis is parallel to the strike of the El Tigre Fault. Jurassic volcano-sedimentary rocks and Upper Palaeocene–Middle Eocene sedimentary strata are absent in the El Palmar High, whereas in the Manuelote Syncline the thickness of those units may reach up to 3.5 km (Maze, 1984) (Fig. 3a). We interpreted the El Tigre Fault as a reactivated structure with a normal component in Jurassic and Palaeocene times, as proposed by Quijada & Cassani (1997).

UPPER CAMPANIAN–LOWER EOCENE SYNOROGENIC CLASTIC SUCCESSION

Lithology, thickness variations and age

In the Ranchería Basin, the Upper Campanian–Lower Eocene succession is characterized by two fine-grained siliciclastic units separated by a mixed calcareous-siliciclastic unit (Figs 5–7).

The upper member of the Colón Formation includes laminated calcareous mudstone and micaceous and carbonaceous mudstone with siderite nodules and planktonic and benthonic foraminifera (Martínez & Hernández, 1992). The thickness of this succession is uniform across the study area, from 500 m in well B in the Ranchería Basin (Caceres *et al.*, 1981) to 480 m in the Manuelote Syncline (Quijada & Cassani, 1997). The base of this unit is dated as upper Campanian (Martínez & Hernández, 1992), whereas the top is lower Palaeocene in age on the basis of foraminifera and pollen assemblages recovered in well B (Figs 4 and 6).

Carbonate and siliciclastic strata of the Hato Nuevo and Manantial units in the Ranchería Basin and the Guasare Formation in the Manuelote Syncline conformably overlie the Colón Formation (Fig. 4). In the Ranchería Basin, the Hato Nuevo Formation includes glauconitic shales and pelecypod- and oyster-rich sandy limestone beds (Fig. 6). Similar lithologies are reported in the Manantial Formation, but shale intervals are thicker, and fine-grained sandstone interbeds are common to the top (Figs 6 and 7). One hundred and ninety metres of the upper Manantial Formation, described in cores from a shallow well (Fig. 7), include at the base upward-coarsening calcareous sandstone and biomicrite beds, followed by a thick succession of wavy, lenticular and planar laminated dark-coloured mudstone and siltstone beds with plant remains and signals of bioturbation. Towards the top, upward-coarsening and upward-fining successions consist of calcareous and fossiliferous sandstone beds interbedded with laminated mudstone and siltstone beds. A local conglomerate bed includes dominantly micritic and biomicritic rock fragments in a sandy calcareous matrix (Appendix S1). The Hato Nuevo and Manantial units thin eastward from >600 m on the surface to <180 m in well A. A lower Palaeocene age is assigned on the basis of foraminifera and pollen assemblages in well B, and mollusc identification in the Cerrejón coal mine (Fig. 4). The 300-mthick Guasare Formation is more calcareous and richer in glauconite, and pollen assemblages recovered in the Paso Diablo coal mine indicate a Lower-to-Upper Palaeocene age.

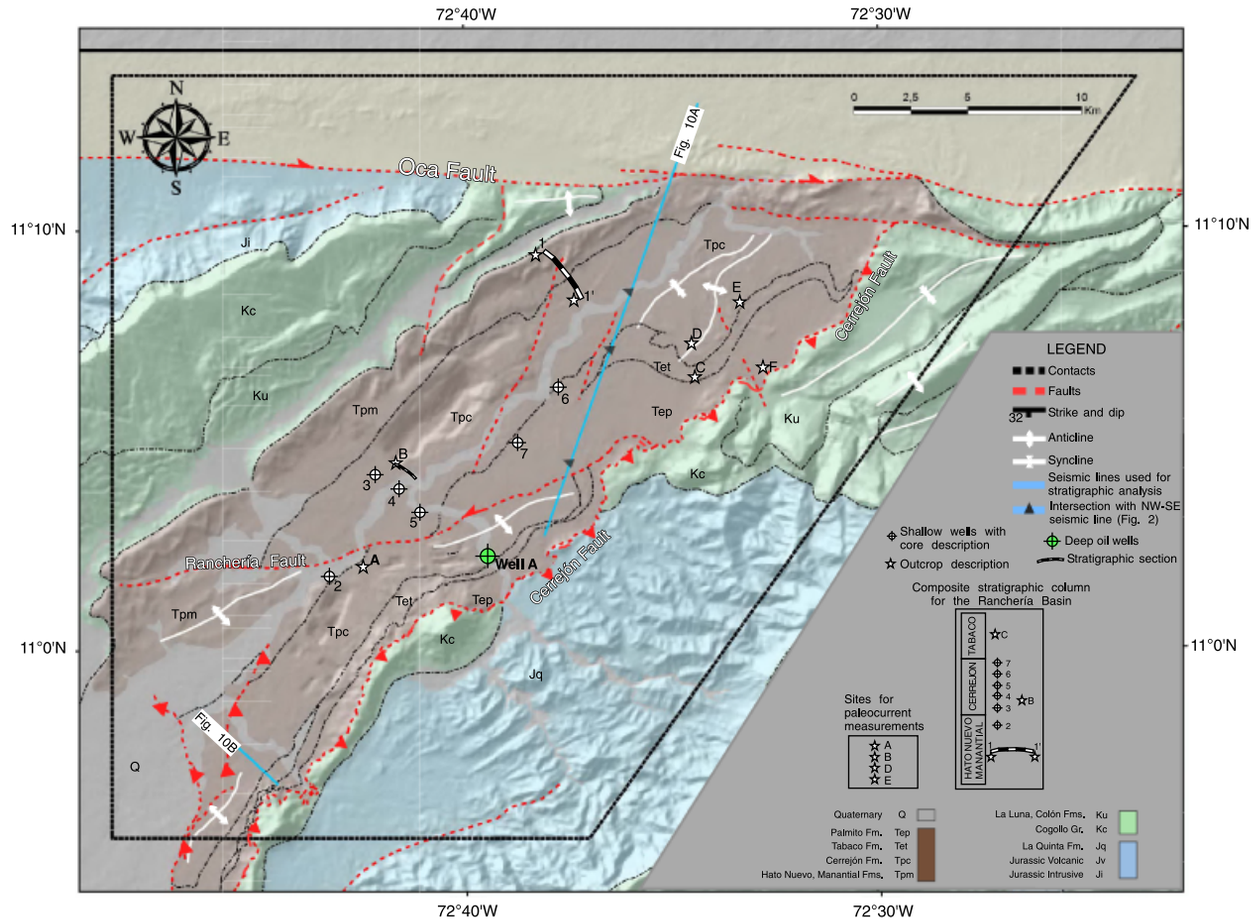

Fig. 5. Location of shallow wells and outcrops used for the construction of the composite stratigraphic sections in the Ranchería Basin, and the two seismic lines used for seismic stratigraphy analysis. Deep oil well A is shown for reference.

In the Ranchería Basin, the middle-to-upper Palaeocene Cerrejón Formation (Jaramillo *et al.*, 2007) overlies the mixed calcareous-siliciclastic Manantial Formation (Fig. 7). The Cerrejón Formation is a 1-km-thick coal-bearing unit that consists of very-fine- to fine-grained argillaceous sandstones, dark-coloured sandy siltstones and interbeds of mudstones, shales and coal seams (Fig. 7). Palynological reports in Well A indicate a Lower Palaeocene age for lowermost Cerrejón Formation.

Vertical lithofacies associations, the lateral continuity and the external geometry of lithological units were documented with the description of cores from six shallow wells (cores of the Cerrejón coal mine) and excellent outcrops left by open mining of the Cerrejón Formation (Figs 5, 7 and 8). Sedimentary successions at the base of the Cerrejón Formation were described in shallow wells 3 and 4, and they consist either of fossiliferous black shales and laminated black mudstones with thin lenticular laminae of sandstones and/or flaser-laminated sandstones; thick coal seams overlie or underlie these successions. Flaser, wavy, ripple and heterolithic lamination are the sedimentary structures observed in sandstone beds of the lower Cerrejón Formation. Towards the top of the shallow well 4, thick, amalgamated channel-like beds with an irregular base are more frequent (Fig. 8a). Sandstone beds at the top have an upward-fining grain size trend, and internal sedimentary structures are trough cross beds and ripple lamination. Few interbeds of massive sandstone beds are present in the lower Cerrejón Formation (Fig. 8a).

Sedimentary successions of the middle Cerrejón Formation were described in shallow well 5 (Figs 5 and 7). Dominant in the middle Cerrejón Formation are thick intervals of fine-grained strata interbedded with coal seams of variable thickness (1–15 m) and tabular sandstone beds (Fig. 8b). Black mudstone and siltstone beds have planar, lenticular and wavy lamination, and bioturbation is more pervasive at the base of well 5. Thin-to-medium sandstone beds with flaser and heterolithic lamination dominate at the base, and both upward-coarsening and upward-fining trends in grain size are common. Sandstone beds are almost absent in the middle of well 5, whereas to the top the thickness of sandstone beds increases up section, although grain size continues to be in the range of very-fine-to-fine sand. Lower contacts of sandstone beds are planar, with no signal of erosion (Fig. 8c). Sandstone beds are internally massive or have the following sedimentary structures changing vertically from base to top: horizontal bedding, trough cross beds and ripple lamination (Fig. 8c).

The upper Cerrejón Formation, described in shallow wells 6 and 7, is dominated by upward-fining successions

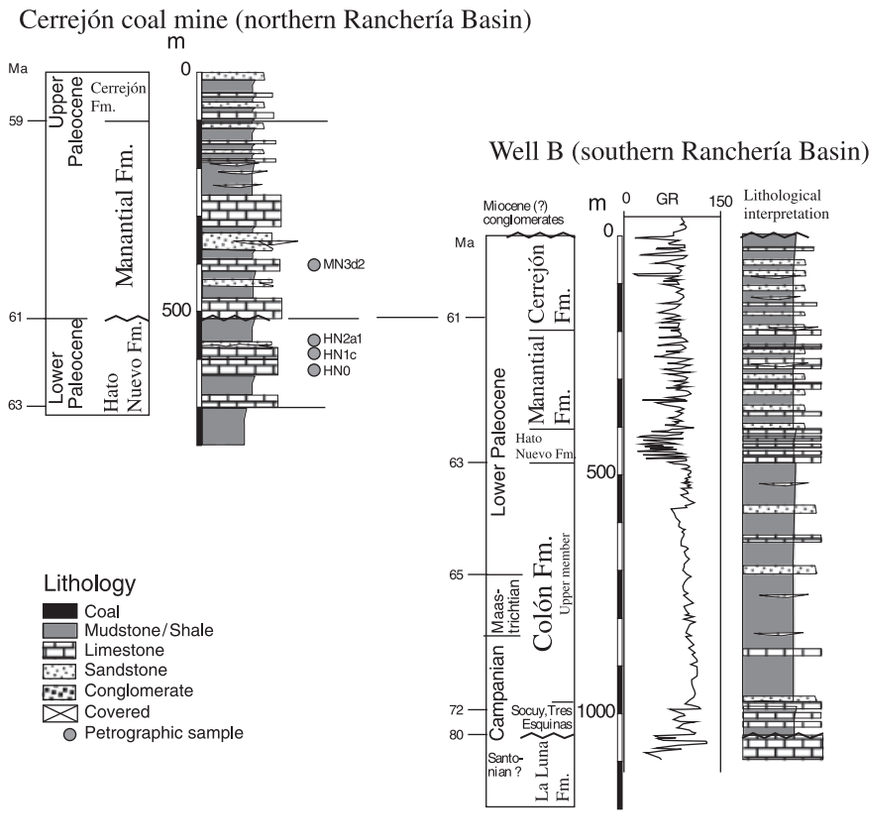

Fig. 6. Left: Generalized stratigraphic columns of Hato Nuevo, Manantial and lower Cerrejón formations in the Cerrejón coal mine (section 1-1′ in Fig. 5) with location of petrographic samples (see raw data of sandstone petrography in Appendix S1). Right: Interpretation of the gamma-ray profile for the Colón to Manantial formations in well B (see location in Fig. 2).

that consist of thick-to-very-thick-bedded sandstone beds (Figs 5 and 7). Grain size trends range from fine sand to granule, including granule-size micritic fragments (Appendix S1). Sandstone beds are internally massive, or include horizontally and cross-bedded sedimentary structures. The external geometry of sandstone beds varies from tabular with planar lower contacts to channel-like beds with irregular lower contact. These sandstone beds grade up section to massive to lenticularly laminated, bioturbated mudstone and siltstone beds with abundant plant remains. Only one metre-scale thick coal seam is exposed at the base of this interval, whereas thin-to-very-thin coal seams are rarely interbedded in the remainder of the section.

Coal seams overlying sandstone and massive mudstone beds and underlying thick successions of shale and laminated mudstone beds have excellent lateral continuity. These laterally continuous coal seams and laminated mudstone beds overlie flooding surfaces, named 1–9 in Fig. 7. The identification of these flooding surfaces in the Cerrejón Formation was additionally supported by geochemical and petrographic data in coal seams (see data in Appendix S2) and recovery of dinoflagellate cysts (Jaramillo *et al.*, 2007).

In the western Maracaibo Basin (Manuelote Syncline), the Marcelina Formation overlies the mixed calcareous-siliciclastic Guasare Formation (Fig. 9). The 500-m-thick upper Palaeocene Marcelina Formation includes several upward-coarsening successions composed, from base to top, of mudstone and coal, siltstone, and very fine-grained tabular sandstone beds with micritic detritus and glauconite (Fig. 9c). Sandstone beds are tabular, and the thickness of such beds increases towards the top of each succession.

Coarse-grained strata unconformably overlie the Cerrejón and Marcelina Formations. In the Ranchería Basin, the Tabaco and Palmito Formations overlie the Cerrejón Formation in angular unconformity. The Tabaco Formation is < 100 m thick and includes varicoloured massive mudstone beds interbedded with cross-bedded conglomeratic sandstone beds (Fig. 7, Appendix S1), whereas the Lower Eocene Palmito Formation (Montes *et al.*, 2010, locality F in Fig. 5) is poorly exposed and includes light-coloured massive mudstones. Similarly, conglomerates, sandstones and mudstones of the uppermost Palaeocene to Middle Eocene Misoa Formation overlie the Upper Paleocene Marcelina Formation (Pardo, 2004). Felsic volcanic tuffs and volcaniclastic sandstones, dated 56 ± 0.03 Ma (Jaramillo et al., 2010), are locally interbedded in the lower Misoa Formation (Fig. 9b).

Depositional environment interpretation

Table 1 summarizes lithological and biological criteria used for depositional interpretation for the Campanian–Lower Eocene succession. The lowermost beds of the Colón Formation are the deposits accumulated in the deepest marine conditions, and the vertical variation of planktonic

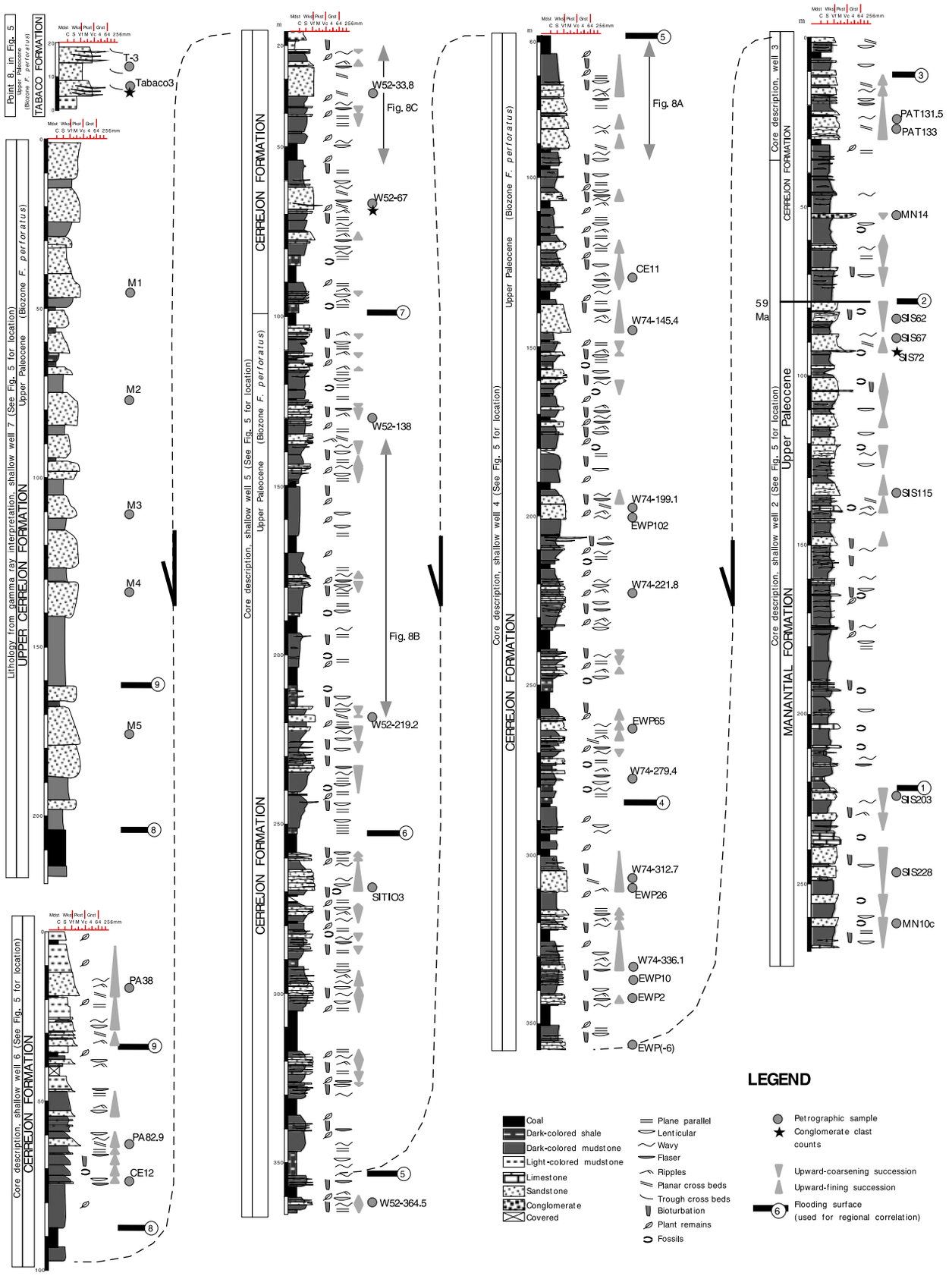

Fig. 7. Composite stratigraphic column of the Manantial, Cerrejón and Tabaco formations in the Cerrejón coal mine, showing the stratigraphic position of samples for sandstone petrography and conglomerate clast counts for provenance analysis (see raw data in Appendix S1). In shallow wells 4 and 5, 207 palynological analysis (Jaramillo *et al.*, 2007), and 53 analysis of organic petrography and chemical composition of coal seams (see raw data in Appendix S2)were carried out.

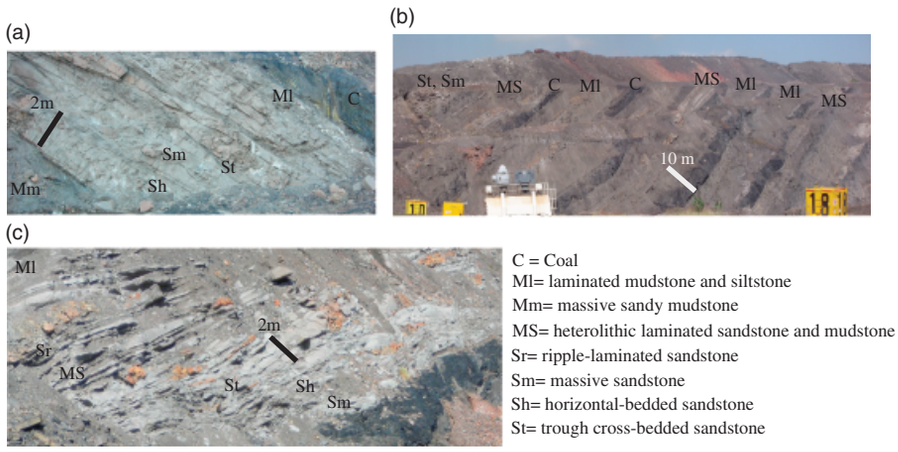

Fig. 8. Lateral geometry and stacking pattern of Cerrejón Formation strata examined in outcrops of the Cerrejón coal mine, and comparison with one-dimensional descriptions of wells presented in Fig. 7. (a) Medium-to-thick bedded, amalgamated sandstone beds overlying with irregular contact massive mudstone beds (strata below surface 5 in well 4). (b) Thick, dark-coloured mudstone and siltstone beds interbedded with coal seams and tabular sandstone beds (strata above surface 6 in well 5). (c) Sharp and non-erosive contact between a thick coal seam (or laminated mudstone in wells) and horizontal-to-massive bedded sandstone (strata above surface 7 in well 5). B and C are examples of strata in aggradational staking patterns, whereas A corresponds to progradational stacking patterns below the flooding surface.

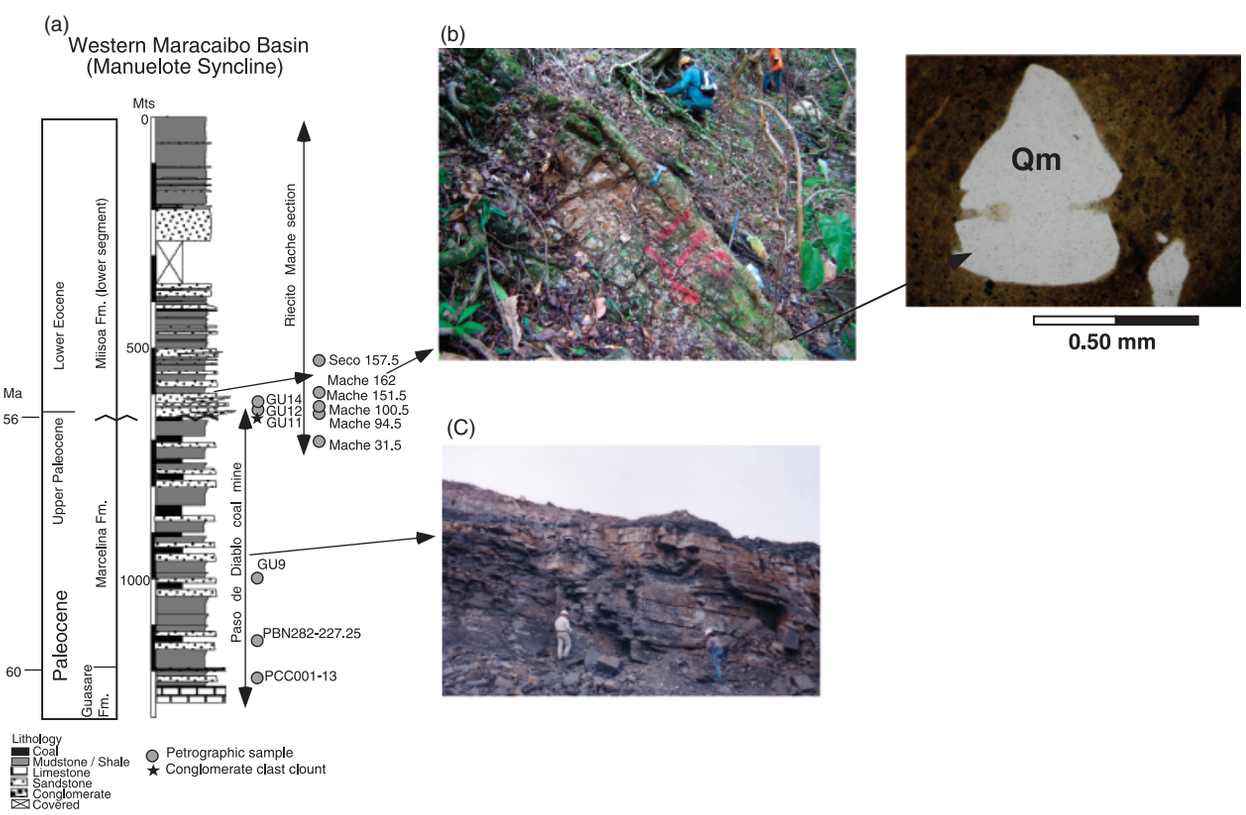

Fig. 9. (a) Composite stratigraphic column of upper Guasare, Marcelina and lower Misoa formations in the Manuelote Syncline (see Fig. 2 for location; uppermost 500 m of the Misoa Fm are descriptions from Pardo, 2004) with location of petrographic samples and conglomerate clast counts (see raw data in Appendix S1). (b) Volcanic felsic tuff interbedded in the lower Misoa Formation with a U-Pb Zircon radiometric age of 56.09 ± 0.03 Ma (Jaramillo et al., 2010). Inset to the right: monocrystalline quartz (Qm) with embaymets surrounded by volcanic glass with slight flow structure (parallel nicols). (c) Tabular geometry of fine-grained calcareous sandstone beds at the top of an upward-coarsening succession.

and benthonic foraminifera supports the interpretation of shallowing water depth within neritic to prodeltaic environments for the upper member of the Colon Formation (Martínez & Hernández, 1992).

Calcareous beds of the Hato Nuevo, Manantial and Guasare Formations indicate a period of continental-ward migration of the shoreline (i.e. marine transgression) and decrease of siliciclastic sediment supply during the Early

Table 1. Depositional environment interpretation

Stratigraphic unit	Lithological association	Bioturbation, fossils, pollen content	Other indicators	Depositional environment
Misoa	Mudstone: massive Sandstone: cross-bedded, conglomerate fragments on cross beds Coal: thin beds Felsic tuffs, volcaniclastic sandstones: massive	Pollen recovery in coal beds		Fluvial floodplains and channels. Nearby volcanic activity
Palmito	Mudstones: light-colored, massive	Poor pollen recovery		Fluvial floodplains
Tabaco	Mudstone: light-colored, massive Sandstone: cross-bedded, conglomerate fragments on cross beds Conglomerate: massive	Poor pollen recovery		Fluvial floodplains and channels
Marcelina	Coal: more abundant and thicker beds in the middle of the unit	Fossils (mollusks?) in few mudstone beds	Reworked micritic fragments	Mouth bars and deltaic plains
	Upward-coarsening successions	Bioturbation	Glauconite	
	Mudstones: lenticular, wavy, plane parallel lamination:	Abundant plant remains		
	Very fine- to fine-grained sandstones: tabular geometry, ripple and plane parallel lamination. Cross-bedded sandstones toward the top of the unit	Good pollen recovery		
Middle and upper Cerrejón (from flooding surface 5 to the top)	Coal: thicker and more abundant beds in the middle Cerrejón (well 5), almost absent in the top (well 7)	Fossils (mollusks?) in few mudstone beds	Reworked micritic fragments	Lacustrine systems Fluvial floodplains, channels, crevasse splays
	Upward-fining and upward-coarsening successions; the former dominates at the top	Bioturbation toward the base		
	Very fine to conglomeratic sandstones: internally massive, or cross-bedded, ripple lamination, channel-like geometries	Abundant plant remains (macroflora)		Hyperconcentrated flows
	Sandy siltstone: dark and light colored, massive, lenticular lamination	Good pollen recovery		
	Mudstone: dark and light colored; massive, lenticular and wavy lamination; plane parallel lamination to the base	Vertebrate fragments (fresh-water turtles, crocodiles, snakes)		
Lower Cerrejón (from the base to flooding surface 5)	Coal: thicker and more abundant beds to the top	Oyster, mollusks in mudstone beds	Increase of sulphur content in coal seams (Ramos, 1990; Layton, 2006)	Lacustrine systems with brackish influence
	Upward-fining successions	Dinoflagellate		Fluvial/coastal floodplains and channels Hyperconcentrated flows
	Very fine- to fine-grained sandstone: internally massive or cross-bedded	Bioturbation		
	Sandy siltstone: dark-colored, massive, or with wavy and lenticular lamination	Abundant plant remains (macroflora)		
	Mudstone: dark-colored, plane parallel, lenticular, wavy lamination	Good pollen recovery		
	Tabular Sandstone beds: ripple, lenticular, flaser lamination	Vertebrate fragments		

Table 1. (Continued)

Stratigraphic unit	Lithological association	Bioturbation, fossils, pollen content	Other indicators	Depositional environment
Guasare	Limestone: massive micrite, biomicrite Mudstone: dark-colored, plane-parallel lamination Calcareous fossiliferous sandstones: ripple lamination	Pelecypod, oyster, mollusks Dinoflagellate Bioturbation	Glauconite	Mixed carbonate-siliciclastic marginal- to shallow-marine platform
Manantial	Upward-coarsening and upward-fining successions Shale: dark-colored, plane-parallel lamination Sandy limestone: massive, wavy lamination Fine-grained sandstone: lenticular, wavy and ripple lamination (more interbeds toward the top) Calcareous fossiliferous sandstones: ripple, wavy lamination	Pelecypod, oyster, mollusks Bioturbation Plant remains Poor pollen recovery	Glauconite	Mixed carbonate-siliciclastic marginal- to shallow-marine platform
Hato Nuevo	Sandy limestone; massive, wavy lamination Shale: dark-colored, laminated	Pelecypod, oyster	Glauconite	Marginal- to shallow-marine platform
Colón (upper member)	Mudstone: dark-colored, plane-parallel lamination, calcareous Mudstone: micaceous and carbonaceous	Planktonic and benthonic foraminifera	Glauconite	Neritic to prodeltaic

Palaeocene. Etayo-Serna (1979) interpreted the Hato Nuevo and Manantial Formations as being accumulated in marginal- to shallow-marine platform environments. The Late Palaeocene age of the uppermost strata of the Guasare Formation indicates the northeastward retreat of marine deposition and diachronous onset of coal-bearing siliciclastic deposition, being older in the Ranchería Basin and younger along the western side of the Maracaibo Basin.

In Late Palaeocene time, the depositional profile with continental settings to the west and marginal settings to the east continued. Lithological, palynofloral and macrofloral associations in the Cerrejón Formation indicate deposition in dominantly continental settings with the development of lacustrine systems with brackish influence. Analyses of fossil plants and vertebrates found in the Cerrejón Formation indicate accumulation in a tropical humid climate (Herrera *et al.*, 2008; Head *et al.*, 2009; Wing *et al.*, 2009). Sandstone beds of the lower Cerrejón Formation represent the transition from coastal to fluvial plains cut by channels towards the top (Fig. 8a). Fine-grained strata and tabular sandstones in the middle Cerrejón Formation record deposition in coastal plains and lacustrine depositional systems (Fig. 8b). Sandstone beds with tabular geometry, nonerosive lower contacts and with sedimentary structures changing up section from massive to horizontal-bedded, and to ripple laminated are indicative of hyperconcentrated flows (Smith & Lowe, 1991) that covered coastal plain settings (Fig. 8c). The dominance of upward-fining sandstone successions to the top of the Cerrejón Formation indicates the prevalence of fluvial channels and floodplain systems during the latest Palaeocene time.

Upward-coarsening successions and coal seams in the Marcelina Formation (Fig. 9c) were deposited in mouth bars and deltaic plains. Sandstone, mudstone and conglomerate beds of the Tabaco, Palmito and Misoa Formations in the Ranchería and western Maracaibo Basins are interpreted as filling of channel structures and fluvial floodplains.

Stratal patterns

Aggradational-to-progradational stacking patterns of deposition are identified for the Colón and Cerrejón Formations. In the upper member of the Colón Formation, Martínez & Hernández (1992) used the increase or decrease of bioturbation and foraminifera content to define the subtle shallowing depositional trend and the aggradational-to-progradational stacking patterns of deposition, despite the homogeneous lithology. In the Cerrejón Formation, flooding surfaces helped in the interpretation of stacking patterns. Flooding surfaces separate amalgamated fluvial sandstones below (e.g. Fig. 8a) from thick mudstone and siltstone beds above. Fine-grained successions above the flooding surface are dark-coloured and laminated in the lower and middle Cerrejón Formation (e.g. flooding surfaces 3–7 in Fig. 7; Fig. 8b), whereas in the upper Cerrejón Formation fine-grained successions

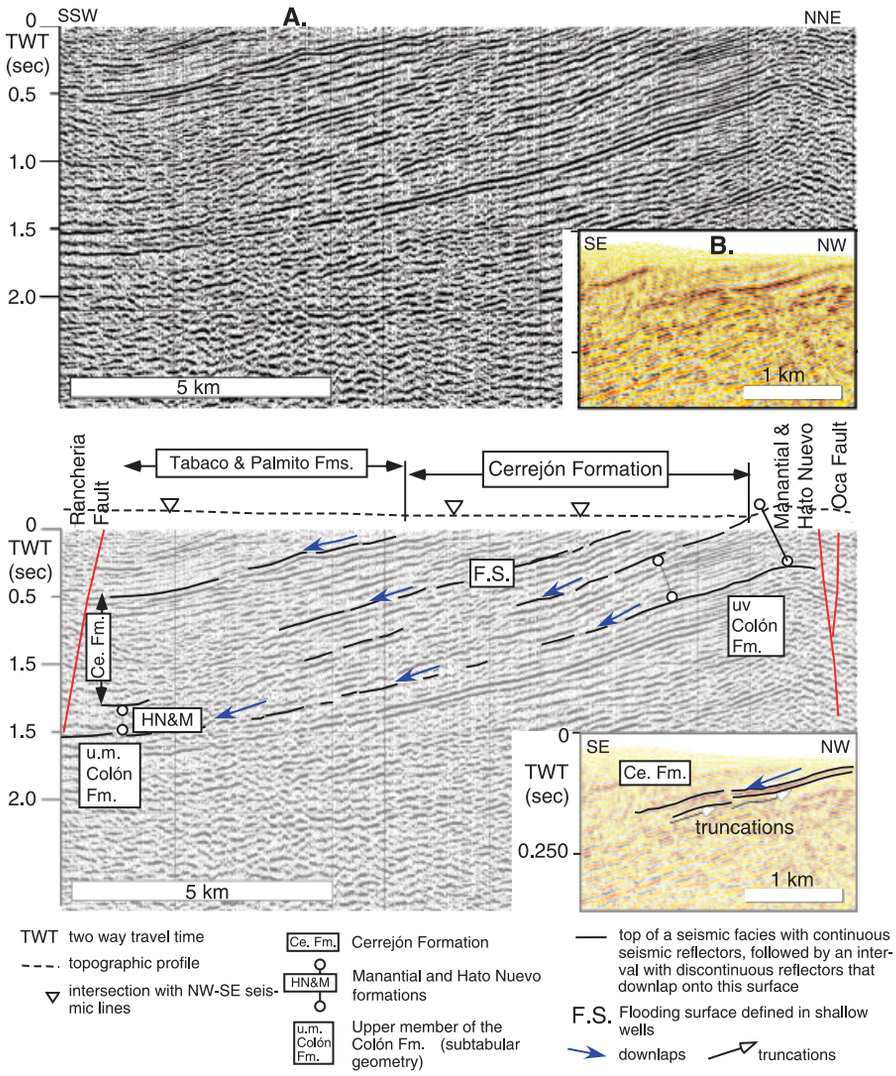

Fig. 10. (a) NNE-striking deep and (b) NW-striking shallow seismic lines showing subsurface stratal geometry of upper member of the Colón Formation, Hato Nuevo, Manantial and Cerrejón formations (see Fig. 5 for location). (a) Two shallow wells were used to control the position of a flooding surface; Well A is located 2.5 km to the SW of the left end of this seismic line. (b) Low-angle angular relations of reflectors within the Cerrejón Formation are identified in shallow seismic lines.

are massive and light-coloured (e.g. flooding surfaces 8 and 9 in Fig. 7). This variation of stacking pattern across flooding surfaces is controlled by the relative rates of generation of accommodation space and sediment supply. Nearly uniform lithological successions in the lower and middle Cerrejón Formation and the prevalence of continental conditions to the top of the Cerrejón Formation, define an aggradational-to-progradational stacking pattern of deposition for this unit.

Two-dimensional stratal geometry and internal truncations of strata were identified using two seismic reflection profiles in little deformed areas (see Figs 5 and 10). Uppermost Cretaceous reflectors identified in well B (Fig. 3b, Line 2) correspond to the upper member of the Colón Formation. These reflectors can be traced to well A, where thicknesses and lithologies of the upper member of the Colón Formation are similar to those in well B. Reflectors above them correspond to the Hato Nuevo and Manantial units and display a downlap relationship with underlying reflectors (Fig. 10a). These calcareous units thin from 620 m in the northwest (Caceres *et al.*, 1980) to <280 m in the south, in wells A and B (Caceres *et al.*, 1981). Seismic reflectors corresponding to the Cerrejón Formation illustrate how the synorogenic clastic wedge advances away from the Santa Marta Massif. Reflectors corresponding to the Cerrejón Formation define downlap relations; the junction of these delineates stratigraphic surfaces that correspond to flooding surfaces (Fig. 10a). Shallow seismic data show low-angle truncation of Cerrejón strata towards the northwest (Fig. 10b).

TECTONIC SUBSIDENCE

Tectonic subsidence profiles from the Ranchería Basin (data from wells A and B, and surface data), Manuelote syncline (data from Quijada & Cassani, 1997) and Cesar Basin (Ayala-Calvo *et al.*, 2009) were used to determine tectonic subsidence signatures (Fig. 11, and Appendix S3 for entry data). The Cesar Basin section represents deposition in the centre of the Lower Cretaceous extensional basin, whereas the other two sections are located in the flanks (Fig. 11).

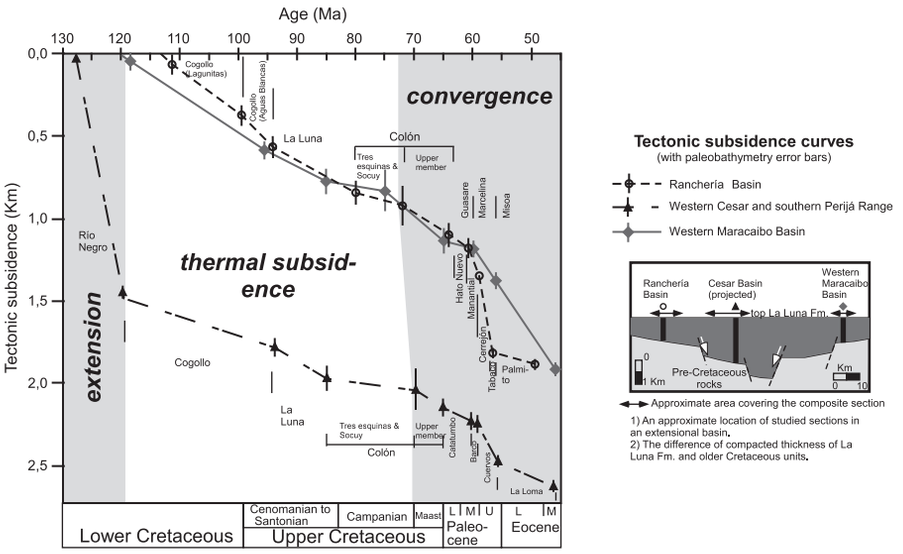

Fig. 11. Comparison of one-dimensional tectonic subsidence curves, allowing the identification of three tectonic subsidence phases: the first related to syn-rift-deposition, the second to a passive-margin regime and the third to a convergent regime. See text for explanation and Appendix S3 for entry data.

The slope of the tectonic subsidence curves shows three different phases of subsidence rates (Fig. 11). Lower Cretaceous units of the Cesar Basin record rapid subsidence during the first phase. The accumulation of the Cogollo Group, La Luna Formation and the lower two members of the Colón Formation correspond to subsidence rates that decrease significantly in time during the second phase. A large increase in tectonic subsidence rates during deposition of the upper member of the Colón Formation (late Campanian–Maastrichtian) characterizes the third phase. A slight decrease in the subsidence rate occurs during accumulation of the shallow-water carbonate Hato Nuevo and Guasare Formations (Early Paleocene) in the Ranchería and western Maracaibo Basins. In the Cesar Basin, the subsidence rate does not change in Early Palaeocene time. The highest subsidence rate of the third phase occurs during the Late Palaeocene, when coal-bearing deposition occurred in all studied areas. Sedimentation continued during the Early to Middle Eocene in the western Maracaibo Basin (Manuelote Syncline) with similar rates of tectonic subsidence of the third segment. In contrast, sedimentation probably ceased in basins adjacent to the Santa Marta Massif (Ranchería and Cesar Basins).

PROVENANCE ANALYSIS

Integration of petrographic and detrital zircon analysis, as well as palaeocurrent data presented in other studies (see Appendix S1 for raw data), allows us to give a comprehensive interpretation of provenance for sandstone units in the Maastrichtian–Lower Eocene succession. Metamorphic lithic fragments of the upper Maastrichtian–Lower Palaeocene sandstones and siltstones reported in the southern Cesar Basin (Ayala-Calvo *et al.*, 2009) and southern Ranchería Basin (Martínez & Hernández, 1992) were supplied from uplifts of the Colombian Central Cordillera to the south and transported to the north by a fluvial-deltaic system in the northern Magdalena Basin (Gómez *et al.*, 2005).

Petrography analyses in the Manantial and Cerrejón Formations indicate an up section increase of feldspars and unstable metamorphic and sedimentary lithic fragments (Fig. 12; raw data in Appendix S1). An up section increase of graphitic and quartz-mica schist fragments, myrmekite fragments, plagioclase, microcline and orthoclase in sandstones of the Manantial and Cerrejón Formations confirms the supply from an igneous-metamorphic source with a thin sedimentary cover. Palaeocurrent indicators measured at three localities near the Tabaco Anticline and one locality to the south of the Ranchería Fault (see Fig. 5 for location of sites) indicate a dominant eastward dispersion for the middle Cerrejón, whereas for the upper Cerrejón they indicate south-southeastward directions (palaeocurrent raw data in Appendix S1). Petrography and palaeocurrent analyses in the Manantial and Cerrejón Formations indicate that the Santa Marta Massif was being eroded during the Palaeocene (Bayona *et al.*, 2007). The unmodified grain-size patterns of sandstones in the Manantial and Cerrejón formations indicate that the distance between the basin and major source areas (Santa Marta Massif) was constant through the Palaeocene.

The high concentration of micritic calcareous fragments in sandstone of the Marcelina Formation, and the local concentration of such clasts in sandstone beds of the upper Cerrejón Formation suggest an additional sediment supply from an exposed shallow carbonate platform, which could correspond to the Guasare carbonate platform that accumulated to the east (Lugo & Mann, 1995; Pardo, 2004).

The association of U/Pb zircon ages in the Cerrejón Formation differs from the association reported in the Manantial Formation (Cardona *et al.*, in press; Fig. 12). Unroofing of the Cretaceous sedimentary cover of the Santa Marta Massif is documented by both the U/Pb zircon ages of 1.0–1.8 Ga reported in the Manantial Formation (i.e. reworking of zircons in Cretaceous beds that were

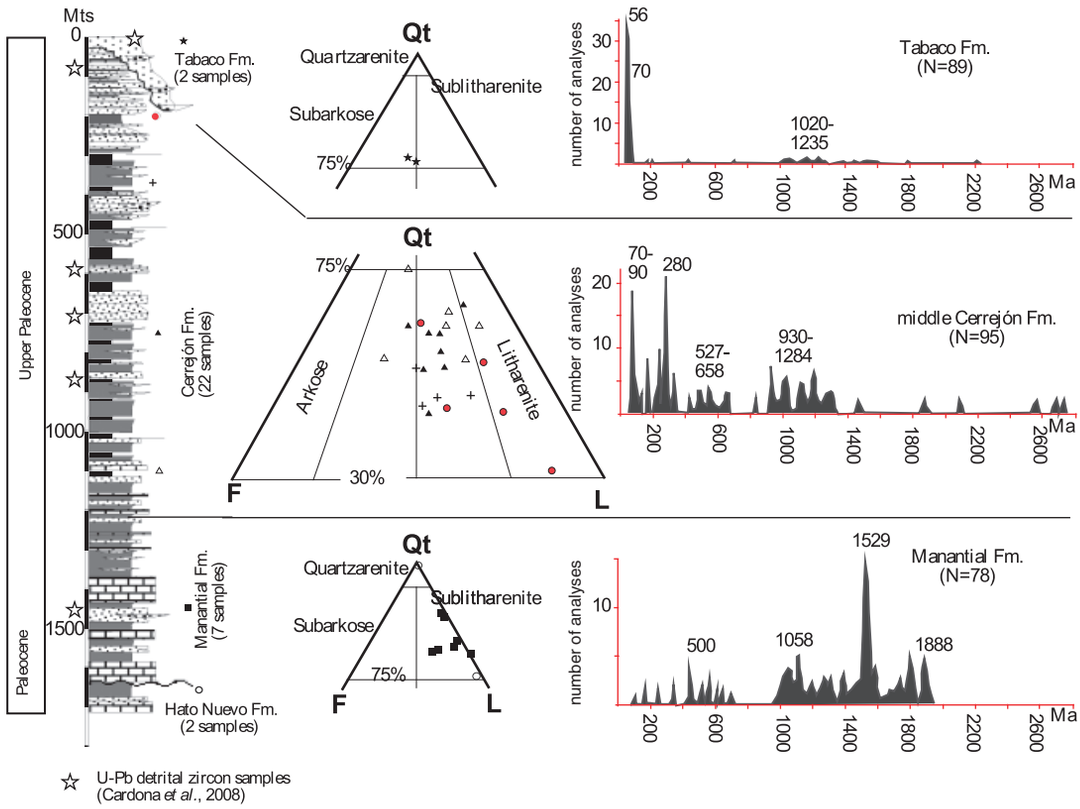

Fig. 12. Compositional trend of Cerrejón and Tabaco sandstone beds, using petrography (see complete dataset and raw data in Appendix S1) and U-Pb detrital zircon population. See text for discussion of provenance for these units.

supplied from the craton) and localized conglomerate beds with a high diversity of carbonate clast types in the Manantial Formation. The age distributions of populations in the Cerrejón Formation suggest that most of the sediments were supplied from the northwestern corner of the massif (Belts I–III in Fig. 1; accreted Cretaceous arc 70–90 Ma +Permo-Triassic rocks 270–280 Ma +Grenvillian basement rocks 930–1200 Ma). Supply from Jurassic plutonic and volcanic rocks, which are dominant in Belt III of the Santa Marta Massif and northern Perijá Range (Fig. 2), is minor during the Palaeocene.

Tabaco and Misoa strata record mixing of detritus derived from both the Perijá Range and Santa Marta Massif (Fig. 12). The abrupt increase of quartzose, chert and sedimentary lithic fragments in sandstone and conglomerate beds of the uppermost Palaeocene–Lower Eocene Tabaco and Misoa formations may be explained by supply from the Perijá Range, which includes several Cretaceous sedimentary units (Fig. 2). The association of both 55–60 Ma and Grenville-age zircons confirms the continuous supply from the magmatic arc and Grenville rocks in the Santa Marta Massif.

DISCUSSION

The internal pattern of deposition and provenance of the upper Campanian–Lower Eocene siliciclastic succession of the Ranchería and Cesar Basins, northern Magdalena and western Maracaibo Basins, needs to be framed in a tectonic environment that explains: (1) whether these basins were connected, and if so, when the study area became fragmented, (2) the changes in patterns of subsidence and (3) uplift patterns of adjacent mountain belts (northern Central Cordillera, the Santa Marta Massif and the Perijá Range) and their relationship to filling of adjacent sedimentary basins.

Two episodes of variation in tectonic subsidence rates affected all studied basins (Fig. 11), the first during the Maastrichtian and the second during the Late Palaeocene–Early Eocene. During the first episode, a regional regression in sedimentary environments, passing from carbonate platforms (La Luna and lower Colón units) to shallower marginal siliciclastic conditions, was recorded in all studied basins. In Early Palaeocene time, the first change in the deposition and subsidence regime is documented: whereas siliciclastic deposition and high tectonic subsidence rates continued to the south, calcareous marginal deposition and a decrease of tectonic subsidence rates as recorded to the north (Ranchería and western Maracaibo Basins) (Fig. 13a). During the second episode, in Late Palaeocene time, continental deposition was established first in western basins (Magdalena, Cesar and Ranchería Basins) and then migrated eastwards, covering the Guasare Platform in latest Palaeocene time. It is only in Early Eocene time that sedimentation rates likely decreased in western basins (Ranchería and Cesar Basins),

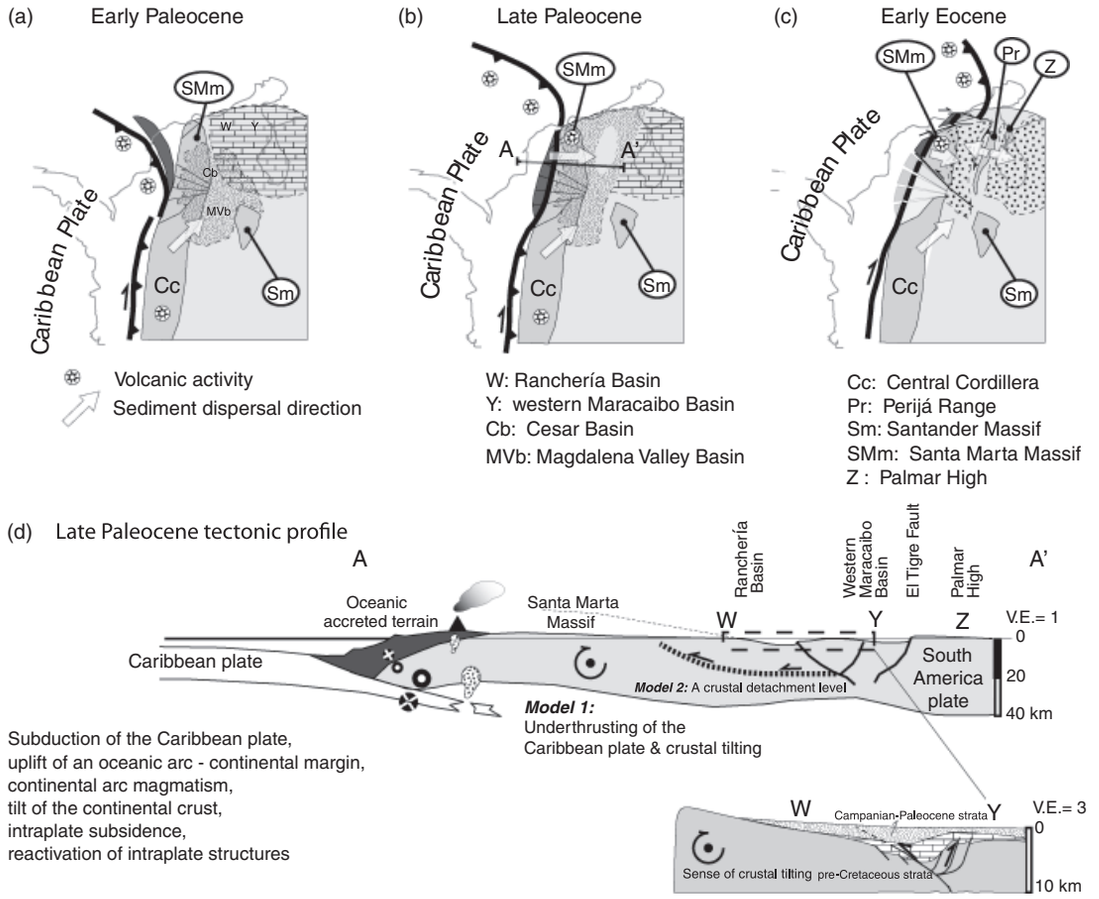

Fig. 13. (a–c) Palaeogeographic maps showing changes in depositional environments and fragmentation of intraplate basins due to diachronous collision, crustal tilting and reactivation of Perijá structures (modified after Montes *et al.*, 2010, and Pindell *et al.*, 1998, 2005). (d) Schematic tectonic profile of the collisional margin in Late Palaeocene time. This diagram illustrates the two models suggested to explain crustal tilting. Lower inset show the geometry of Campanian–Palaeocene units due to extensional tectonism, Maastrichtian–Palaeocene tilting of the Santa Marta Massif and onset of fault reactivation of the Perijá Range.

whereas thick continental deposition continued in the western Maracaibo Basin.

The increase in tectonic subsidence rates and the depositional regression trend recorded in intraplate basins can be related to the diachronous collision of Caribbean segments (Pindell *et al.*, 1998, 2005; Pindell & Kennan, 2009) along the northwestern edge of the South America plate (Central Cordillera and Santa Marta Massif) (Fig. 13). Maastrichtian oblique collision along the margin of the Santa Marta Massif of the Caribbean magmatic arcs (Cardona *et al.*, 2010, in press) coincides with an increase in tectonic subsidence. The supply of metamorphic rock fragments in the Colón Formation (Martínez & Hernández, 1992) and the association of Cretaceous and Palaeozoic detrital zircon ages in the Cerrejón Formation suggest that the western edges of the Santa Marta Massif and Central Cordillera were the source areas. Late Campanian uplift in the Central Cordillera was followed by increased tectonic subsidence rates and continuous sedimentation in the northern Magdalena (Gómez *et al.*, 2005) and Cesar Basins in Maastrichtian–Early Palaeocene time (e.g. Catatumbo Formation in the Cesar Basin, Ayala-Calvo *et al.*, 2009).

Deformation along the Paleocene collisional margin (western edges of the Santa Marta Massif and Central Cordillera) generated topographic relief along the western margin of the South America Plate (Fig. 13a). The large distance between the deformation front and the border of the syntectonic basin, and the constant distance between uplifted blocks and basin depocenter, explain the uniform and immature fine-grained nature of the sandstones in the Colón, Manantial and Cerrejón Formations in the Ranchería Basin; the Catatumbo and Cuervos Formations in the Cesar Basin (Ayala-Calvo *et al.*, 2009); and the Umir and Lisama Formations in the northern Middle Magdalena (Villamil, 1999; Gómez *et al.*, 2005) (Fig. 13a and b). Strong precipitation in the Palaeocene (Head *et al.*, 2009; Wing *et al.*, 2009) favoured rapid transport from source areas to the basin, such as the hyperconcentrated flows documented in the Cerrejón Formation (Fig. 8c). Chronostratigraphic correlations and seismic data presented in this paper support the eastward advance of the synorogenic clastic wedge away from the Palaeocene collisional margin, as proposed by Villamil (1999) and Pardo (2004) (Fig. 13b).

The distal location of the deformation front, the structural continuity between the Santa Marta Massif and the Ranchería Basin and the absence of detrital zircons from adjacent Jurassic rocks preclude a western loading and foreland basin development. A model of crustal-scale tilting of the continental margin, as illustrated in Fig. 13d, better explains the distal and constant location of the deformation front, and the constant distance between source areas and basin. Spatial and temporal variation in rates of crustal tilting may influence the aggradational-to-progradational stacking patterns of deposition along the eastern edge of the tilted crustal block (i.e. the Ranchería and Cesar Basins). Low rates of crustal tilting (or tectonic subsidence) favoured eastward migration of fluvial depositional settings, channel amalgamation (Fig. 8a) and truncations of siliciclastic Palaeocene strata (Fig. 10b). High rates of crustal tilting generated more accommodation space, driving fluvial depositional systems towards emerged blocks and favouring fine-grained coastal and lacustrine deposition towards more subsident blocks (Fig. 8b).

Two different tectonic models could explain the tilting of a rigid continental crust. One model, proposed by Pindell *et al.* (2005) to explain the uplift of the northern Central Cordillera, considers that tilting of the crust could be the product of arc–continent collision, uplift of oceanic and crustal rocks along the collisional margin and the underthrusting of oceanic fragments (Model 1 in Fig. 13d). Incipient low-angle subduction of a buoyant, young and hot Caribbean Plate (see Pindell *et al.*, 2005) may explain the Palaeogene continental-arc magmatism (Cardona *et al.*, in press); an explanation of magmatic activity as far as the eastern margin of the Perijá Range (Fig. 9b) still remains uncertain. The other model, as illustrated by crustal-scale cross sections of Kellogg & Bonini (1982) and Cediel *et al.* (2003), suggests that eastward tilting is due to the northwestward propagation of a crustal-scale, shallow-dipping thrust sheet forming a piggy-back basin (e.g. Talling *et al.*, 1995) (Model 2 in Fig. 13d). Our work does not provide data to constrain the structure of the deep crust, which are needed to evaluate both models. Surface geologic mapping; however, has not identified a northwest-verging, shallow-dipping middle-to-lower-crustal fault in the Santa Marta Massif (Tschanz *et al.*, 1974), as expected for the second model. A regional dip of 16 degrees, as measured in the southeastern flank of the Santa Marta Massif (Montes *et al.*, 2010), would imply the presence of a ramp reaching the surface within the Jurassic plutonic rocks (southeastern Belt III) of the Santa Marta Massif (Model 2 of Fig. 13d), which has not as yet been mapped.

Fault reactivation can be mechanically related to crustal tilting, as these structures bound the southeastern end of the tilted crustal block (Fig. 13c and d). Uplift of the Santander Massif since the Early Palaeocene (Fabre, 1981; Bayona *et al.*, 2008; Ayala-Calvo *et al.*, 2009) and the western flank of the Perijá Range in the Late Palaeocene (Fig. 13c) were the distal responses of intraplate weak structures to the diachronous collision along the plate margin. Early Eocene fault reactivation involved Guasare platform rocks, which supplied carbonate granule-size fragments to the west (Ranchería Basin) and to the east (western Maracaibo Basin), and fragmented depositional systems of the Palaeocene basin (Fig. 13c). The El Tigre Fault in the eastern flank of the Perijá Range reactivated as a normal fault (Fig. 13d). This reactivated structure controlled depositional patterns, composition and stacking pattern of the Upper Palaeocene and Lower Eocene Marcelina and Misoa strata in the down-thrown block, and erosion in the up-thrown block (El Palmar High).

Crustal-scale tilting of a collided margin has been documented farther south in the Ecuadorean Andes, where accretion of oceanic exotic terranes and tectonic underplating of oceanic fragments appear to have caused tectonic uplift by tilting crustal blocks (Jaillard *et al.*, 2002, 2008) and controlled Campanian–Eocene clastic deposition to the East (Toro-Alava & Jaillard, 2005). In the Salar de Atacama Basin in northern Chile, Palaeocene deformation has been associated with eastward crustal-scale tilting (Gómez *et al.*, 2005), suggesting that this mechanism of deformation occurred at different latitudes of the western margin of South America during the Palaeocene. Similar conditions may apply to intraplate basins adjacent to the complex collisional plate margin of northern Papua New Guinea (Abbott *et al.*, 1994). Analogue models presented by Espurt *et al.* (2008) illustrate how the onset of subduction of a thick and buoyant oceanic crust causes first the uplift adjacent to the collisional margin and then subsidence in intraplate settings. As subduction flattens, arc magmatism migrates inboard and later structures in the back-arc region become active.

CONCLUSIONS

The Maastrichtian-to-late Palaeocene basin configuration of the Ranchería Basin was controlled primarily by tectonic subsidence due to crustal-scale tilting, rapid processes of deposition and burial and high rates of sediment supply. These processes were associated with the accretion of oceanic arc terranes along the northwestern corner of South America, which caused the diachronous uplift, and eastward tilting of the northern Central Cordillera and northwestern segment of the Santa Marta Massif. The tectonic evolution described above also drove (1) the generation of accommodation space and aggradational-to-progradational pattern of deposition of the Maastrichtian-to-Lower Eocene succession, (2) continental accumulation of the Maastrichtian-to-Paleocene synorogenic succession in the northern Middle Magdalena, Cesar and western Maracaibo Basins and (3) the reactivation of intraplate structures, which fragmented the Paleocene basin and controlled deposition/uplift in distal parts of the basin. The proposed tectonic model of low-angle subduction of the Caribbean Plate and tilting of a rigid crustal block explains the uplift of an arc–continent collided margin, inboard continental-arc magmatism, tectonic subsidence in an intraplate basin resting on a tilted continental crustal block and reactivation of intraplate structures (Fig. 13d).

ACKNOWLEGEMENTS

Carbones del Cerrejón supplied field and travel expenses for this research, as well as the access to surface and subsurface data from 2004 to 2007. We thank Carbones del Guasare S.A. for access to surface and subsurface data in the Paso Diablo coal mine. Additional financial support for this project comes from Corporación Geológica ARES and the Smithsonian Tropical Research Institute. We thank Omar Montenegro and Carolina Ojeda for analysing petrographic samples of the uppermost Cerrejón Formation, Hernando Mahecha and John Rico for designing some figures and Natasha Atkins for editorial corrections. We also thank the Agencia Nacional de Hidrocarburos and Carbones del Cerrejón for permission to publish seismic lines and for access to biostratigraphic data for Well B. We acknowledge comments and suggestions of Etienne Jaillard, James Pindell, Peter DeCelles, Andrea Fildani and an anonymous reviewer on an earlier version of this manuscript, which greatly improved the content of this manuscript. We appreciate the detailed editorial suggestions and comments of the editor, Peter van der Beek, which helped to improve the presentation of data and ideas.

SUPPORTING INFORMATION

Additional Supporting Information may be found in the online version of this article:

Appendix S1. Sandstone petrography, detrital zircon geochronology and palaeocurrent indicators: methods and raw data. Petrographic, conglomerate counts and data of palaeocurrent indicators for provenance analyses are presented in three figures (A1, A2, A3) and two tables (Tables A1 & A2).

Appendix S2. Organic petrography and chemical composition of coal seams. Data are presented in one figure (B1) and one table (Table B1).

Appendix S3. Entry data for tectonic subsidence analysis. Data are presented in Table C1.

REFERENCES

Abbott, L.D., Silver, E.A., Thompson, P.R., Filewicz, M.V., Schneider, C. & Abdoerrias (1994) Stratigraphic constraints on the development and timing of Arc-continent collision in Northern Papua New Guinea. *J. Sediment. Res.*, **B64**, 169–183.

Acton, G.D., Galbrun, B. & King, J.W. (2000) Paleolatitude of the Caribbean Plate since the Late Cretaceous. In: *Proceedings of the Ocean Drilling Program, Scientific Results* (Ed. by R.M. Leckie, H. Sigurdsson, G.D. Acton & G. Draper). **165**, 149–173. Texas A&M University, College Station, TX.

Allen, P. & Allen, J. (1992) *Basin Analysis, Principles and Applications*. Blackwell Scientific Publications, London.

Alvarez, W. (1971) Fragmented Andean belt of Northern Colombia. In: *Caribbean Geophysical, Tectonic, and Petrologic Studies* (Ed. by T.W. Donnelly), *Geol. Soc. Am., Mem.,* **130**, 71–96.

Ayala-Calvo, C., Bayona, G., Ojeda-Marulanda, C., Cardona, A., Valencia, V., Padrón, C., Yoris, F., Mesa-Salamanca, J. & García, A. (2009) Estratigrafía y procedencia de las unidades comprendidas entre el Campaniano y el Paleógeno en la subcuenca de Cesar – Aportes a la evolución tectónica del área. *Geol. Colomb.*, **34**, 3–33.

Bayona, G., Cortes, M., Jaramillo, C., Ojeda, G., Aristizabal, J. & Reyes-Harker, A. (2008) An integrated analysis of an Orogen-sedimentary basin pair: latest Cretaceous-Cenozoic evolution of the linked Eastern Cordillera Orogen and the Llanos Foreland basin of Colombia. *Geol. Soc. Am. Bull.*, **120**, 1171–1197.

Bayona, G., Lamus, F., Cardona, A., Jaramillo, C., Montes, C. & Tchegliakova, N. (2007) Procesos Orogénicos Del Paleoceno Para La Cuenca De Ranchería (Guajira, Colombia) Definidos Por Análisis De Procedencia. *Geol. Colomb.*, **32**, 21–46.

Beaumont, C., Quinlan, G. & Hamilton, J. (1988) Orogeny and stratigraphy: numerical models of the Paleozoic in the Eastern Interior of North America. *Tectonics*, **7**, 389–416.

Bellizzia, G.A., Pimentel, M.N. & Bajo, O.R. (1976) Mapa Geológico Estructural De Venezuela. Plancha Nc-18-I Manchiques, Foninves. Caracas, Venezuela.

Bioss (1995) Estudio Bioestratigrafico De Muestras De Los Pozos Molino-1x Y Molino-1, Cuenca Del Cesar-Ranchería (Con 2 Anexos). Reporte interno de ECOPETROL, Bogota.

Burke, K. (1988) Tectonic evolution of the Caribbean. *Annu. Rev. Earth Planet. Sci.*, **16**, 201–230.

Caceres, C., Molina, J. & Bernal, J. (1981) Informe Geologico Final Pozo: El Molino 1X, Reporte interno de ECOPETROL S.A. Bogota.

Caceres, H., Camacho, R. & Reyes, J. (1980) The geology of the Ranchería basin. In: *Geological Field-Trips, Colombia 1980–1989* (Ed. by Geotec), pp. 1–31. Asociación Colombiana de Geólogos y Geofísicos del Petróleo, Bogotá.

Cardona, A., Valencia, V., Bayona, G., Duque, J., Ducea, M., Gerhels, G., Jaramillo, C., Montes, C., Ojeda, G. & Ruiz, J. (in press) Early subduction orogeny in the Northern Andes: Turonian to Eocene magmatic and provenance record in the Santa Marta massif and Rancheria Basin, Northern Colombia. *Terranova*.

Cardona, A., Valencia, V.A., Bustamante, C., Garcia-Casco, A., Ojeda, G., Ruiz, J., Saldarriaga, M. & Weber, M. (2010) Tectonomagmatic setting and provenance of the Santa Marta schist, northern Colombia: insights on the growth and approach of Cretaceous Caribbean oceanic terranes to the South American continent. *J. S. Am. Earth Sci.*, **29**, 784–804; doi: 10.1016/j.jsames.2009.08.012.

Cardona-Molina, A., Cordani, U. & MacDonald, W.D. (2006) Tectonic correlations of Pre-Mesozoic crust from the Northern Termination of the Colombian Andes, Caribbean region. *J. S. Am. Earth Sci.*, **21**, 337–354.

Cediel, F., Shaw, R. & Caceres, C. (2003) Tectonic assembly of the Northern Andean block. In: *The Circum-Gulf of Mexico and the Caribbean: Hydrocarbon Habitats, Basin Formation and Plate Tectonics* (Ed. by C. Bartolini, R. Buffler & J. Blickwede), *Am. Assoc. Petrol. Geol. Mem.* **79**, 815–848.

Cordani, U., Cardona, A., Jimenez, D., Liu, D. & Nutman, A. (2005) Geochronology of Proterozoic Basement Inliers from the Colombian Andes: tectonic history of Remnants from a Fragmented Grenville belt. In: *Terrane Processes at the Margins of Gondwana* (Ed. by A.P.M. Vaughan, P.T. Leat & R.J. Pankhurst), *Geol. Soc. Lond., Spec. Publ.,* **246**, 329–346.

Dasch, L.E. (1982) U–Pb Geochronology of the Sierra De Perijá, Venezuela. Master Thesis, Case Western Reserve University.

DeCelles, P. & Giles, K. (1996) Foreland basin systems. *Basin Res.*, **8**, 105–123.

Duerto, L., Escalona, A. & Mann, P. (2006) Deep structure of the Mérida Andes and Sierra De Perijá Mountain Fronts, Maracaibo Basin, Venezuela. *AAPG Bull.*, **90**, 505–528.

Escalona, A. & Mann, P. (2006) Tectonic controls of the right-lateral Burro Negro tear fault on Paleogene structure and stratigraphy, northeastern Maracaibo Basin. *AAPG Bull.*, **90**, 479–504.

Espurt, N., Funiciello, F., Martinod, J., Guillaume, B., Regard, V., Faccenna, C. & Brusset, S. (2008) Flat subduction dynamics and deformation of the South American plate: insights from analog modeling. *Tectonics*, **27**, TC3011, doi: 10.1029/2007TC002175.

Etayo-Serna, F. (1979) Moluscos De Una Capa Del Paleoceno De Manantial (Guajira). *Bol. Geol. Univ. Ind. Santander*, **13**(27), 5–55.

Fabre, A. (1981) Estratigrafía De La Sierra Nevada Del Cocuy, Boyacá Y Arauca, Cordillera Oriental (Colombia). *Geol. Norand.*, **4**, 3–12.

Fildani, A., Hessler, A., Graham, S. (2008) Trench-forearc interactions reflected in the sedimentary fill of Talara basin, northwestern Peru. *Basin Research*, **20**, 305–331; doi: 10.1111/j.1365-2117.2007.00346.x.

Forero, A. (1990) The basement of the Eastern Cordillera, Colombia: an Allochthonous Terrane in Northwestern South America. *J. S. Am. Earth Sci.*, **3**, 141–151.

Gawthorpe, R. & Leeder, M. (2000) Tectono-sedimentary evolution of active extensional basins. *Basin Res.*, **12**, 195–218.

Gómez, E., Jordan, T., Allmendinger, R.W., Hegarty, K. & Kelley, S. (2005) Syntectonic Cenozoic sedimentation in the Northern Middle Magdalena valley basin of Colombia and implications for exhumation of the Northern Andes. *Geol. Soc. Am. Bull.*, **117**, 547–569; doi: 510.1130/B25454.25451.

Haq, B.U., Hardenbol, J. & Vail, P. (1987) Chronology of fluctuating sea levels since the Triassic. *Science*, **235**, 1156–1166.

Head, J., Bloch, J., Hasting, A., Bourque, J., Cadena, E., Herrera, F., Polly, P.D. & Jaramillo, C. (2009) Giant Boine snake from a Paleocene Neotropical rainforest indicates Hotter past equatorial temperatures. *Nature*, **457**, 715–718.

Herrera, F., Jaramillo, C., Dilcher, D., Wing, S.L. & Gómez, C. (2008) Fossil Araceae from a Paleocene neotropical rainforest in Colombia. *Am. J. Botany*, **95**, 1569–1583.

Hoorn, C. & Wesselingh, F. (2010) Editors *Amazonia, Landscape and Species Evolution: A Look into the Past*. Wiley-Blackwell, New York.

Jaillard, E.P., Bengtson, P., Ordonez, M., Vaca, W., Dhondt, A., Suarez, J. & Toro, J. (2008) Sedimentary record of terminal Cretaceous Accretions in Ecuador: the Yunguilla group in the Cuenca area. *J. S. Am. Earth Sci.*, **25**, 133–144.

Jaillard, E.P., Herail, G., Monfret, T. & Worner, G. (2002) Andean geodynamics: main issues and contributions from the 4th ISAG, Göttingen. *Tectonophysics*, **345**, 1–15.

Jaillard, E.P., Lapierre, H., Ordoñez, M., Toro-Avala, J., Amórtegui, A. & Vanmelle, J. (2009) Accreted oceanic terranes in Ecuador: southern edge of the Caribbean plate? In: *The Origin and Evolution of the Caribbean Plate* (Ed. by K.H. James, M.A. Lorente & J.L. Pindell), *Geol. Soc. Lond., Spec. Publ.*, **328**, 469–485.

Jaramillo, C., Ochoa, D., Contreras, L., Pagani, M., Carvajal-ortiz, H., Pratt, L.M., Krishnan, S., Cardona, A., Romero, M., Quiroz, L., Rodriguez, G., Rueda, M.J., De La Parra, F., Moron, S., Green, W., Bayona, G., Montes, C., Quintero, O., Ramirez, R., Mora, G., Schouten, S., Bermudez, H., Navarrete, R., Parra, F., Alvarán, M., Osorno, J., Crowley, J.L., Valencia, V. & Vervoort, J. (2010) Effects of Rapid Global Warming at the Paleocene-Eocene Boundary on Neotropical Vegetation. *Science*, **330**, 957–961; doi: 10.1126/Science.1193833.

Jaramillo, C., Pardo, A., Rueda, M., Harrington, G., Bayona, G., Torres, V. & Mora, G. (2007) Palynology of the Upper Paleocene Cerrejón formation, Northern Colombia. *Palynology*, **31**, 153–189.

Jaramillo, C., Rueda, M. & Torres, V. (in press) A Palynological zonation for the Cenozoic of the Llanos and Llanos Foothills of Colombia. *Palynology*.

Jordan, T. & Flemings, P.B. (1991) Large-scale stratigraphic architecture, Eustatic variation, and unsteady Tectonism: a theoretical evaluation. *J. Geophys. Res.*, **96**(B4), 6681–6699.

Kellogg, J. (1984) Cenozoic tectonic history of the Sierra de Perijá, Venezuela-Colombia, and adjacent basins. In: *The Caribbean-South American Plate Boundary and Regional Tectonics* (Ed. by W.E. Bonini, R.B. Hargraves & R. Shagam), *Geol. Soc. Am. Mem.*, **162**, 239–261.

Kellogg, J. & Bonini, J. (1982) Subduction of the Caribbean plate and Basement uplifts in the overriding South America plate. *Tectonics*, **1**, 251–276.

Lister, G.S., Etheridge, M.A. & Symonds, P.A. (1986) Detachment faulting and the evolution of passive continental margins. *Geology*, **14**, 246–250.

Lugo, J. & Mann, P. (1995) Jurassic–Eocene tectonic evolution of Maracaibo Basin, Venezuela. In: *Petroleum Basins of South America* (Ed. by A.J. Tankard, R.S. Suárez & H.J. Welsink), *AAPG Mem.* **62** , 699–725. Tulsa, Oklahoma.

MacDonald, D., Doolan, B. & Cordani, U. (1971) Cretaceous-early tertiary metamorphic age values from the South Caribbean. *Geol. Soc. Am. Bull.*, **82**, 1381–1388.

Martínez, J. & Hernández, R. (1992) Evolution and drowning of the late Cretaceous Venezuelan carbonate platform. *J. S. Am. Earth Sci.*, **5**, 197–210.

Maze, W.B. (1984) Jurassic La Quinta Formation in the Sierra De Perijá, Northwestern Venezuela; geology and Tectonic environment of Red beds and Volcanic rocks. In: *The Caribbean-South American Plate Boundary and Regional Tectonics* (Ed. by W.E. Bonini, R.B. Hargraves & R. Shagam), *Geol. Soc. Am. Mem.*, **162**, 263–282.

McKenzie, D. (1978) Some remarks on the development of sedimentary basins. *Earth Planet. Sci. Lett.*, **40**, 25–32.

Miller, J.B. (1962) Tectonic trends in Sierra De Perijá and adjacent parts of Venezuela and Colombia. *AAPG Bull.*, **46**, 1565–1595.

Montes, C., Guzman, G., Bayona, G., Cardona, A., Valencia, V. & Jaramillo, C.A. (2010) Clockwise Rotation of the Santa Marta Massif and Simultaneous Paleogene to Neogene Deformation of the Plato-San Jorge and Cesar-Ranchería Basins. *J. S. Am. Earth Sci.*, **29**, 832–848, doi: 10.1016/j.jsames.2009.07.010.

Pardo, A. (2004) Paleocene–eocene palynology and palynofacies from Northeastern Colombia and Western Venezuela. PhD Thesis, Universite de Liege.

Pindell, J.L., Higgs, R. & Dewey, J. (1998) Cenozoic Palinspastic reconstruction, Paleogeographic evolution and hydrocarbon setting of the Northern Margin of South America. In: *Paleogeographic Evolution and Non-Glacial Eustasy, Northern South America* (Ed. by J. Pindell & C. Drake), *SEPM Spec. Publ.* **58**, 45–84.

Pindell, J.L. & Kennan, L. (2009) Tectonic evolution of the Gulf of Mexico, Caribbean and northern South America in the mantle reference frame: an update. In: *The Origin and*

Evolution of the Caribbean Plate (Ed. by K.H. James, M.A. Lorente & J.L. Pindell), *Geol. Soc. Lond., Spec. Publ.* **328**, 1–55.

Pindell, J.L., Kennan, L., Maresch, W.V., Stanek, K.P., Draper, G. & Higgs, R. (2005) Plate kinematics and crustal dynamics of circum-Caribbean arc-continent interactions: tectonic controls on basin development in Proto-Caribbean margins. In: *Caribbean–South American Plate Interactions, Venezuela* (Ed. by H.G. Ave Lallemant & V.B. Sisson), *Geol. Soc. Am. Spec. Pap.,* **394**, 7–52.

Quijada, E. & Cassani, F. (1997). Tectonismo E Historia Termal Durante El Paleógeno Temprano En El Area Norte De La Sierra De Perijá, Venezuela Occidental. VI Simposio Bolivariano, Cartagena, Colombia, ACGGP.

Restrepo-Pace, P., Ruiz, J., Gehrels, G. & Cosca, M. (1997) Geochronology and Nd Isotopic data of Grenville-age rocks in the Colombian Andes: new constraints for late Proterozoic-early Paleozoic Paleocontinental reconstructions of the Americas. *Earth Planet. Sci. Lett.*, **150**, 427–441.

Sinclair, H.D. (1997) Tectonostratigraphic model for underfilled peripheral foreland basins: an alpine perspective. *Geol. Soc. Am. Bull.*, **109**, 324–346.

Smith, G.A. & Lowe, D.R. (1991) Lahars: volcano-hydrologic events and deposition in the Debris flow – hyperconcentrated flow continuum. In: *Sedimentation in Volcanic Settings* (Ed. by R.V. Fisher & G.A. Smith), *SEPM Spec. Publ.* **45**, 59–87.

Talling, P.J., Lawton, T., Burbank, D.W. & Hobbs, R.S. (1995) Evolution of latest Cretaceous-Eocene Nonmarine Deposystems in the Axhandle Piggyback basin of Central Utah. *Geol. Soc. Am. Bull.*, **107**, 297–315.

Toro-Alava, J. & Jaillard, E.P. (2005) Provenance of the Upper Cretaceous to Upper Eocene Clastic sediments of the Western Cordillera of Ecuador. *Tectonophysics*, **399**, 279–292.

Tschanz, C., Marvin, R., Cruz, J., Mennert, H. & Cebula, E. (1974) Geologic evolution of the Sierra Nevada De Santa Marta. *Geol. Soc. Am. Bull.*, **85**, 269–276.

Ujueta, G. & Llinás, R.D. (1992) Reconocimiento Geológico De La Parte Mas Septentrional De La Sierra De Perijá. *Geol. Colomb.*, **17**, 197–209.

Villamil, T. (1999) Campanian-Miocene Tectonostratigraphy, Depocenter evolution and basin development of Colombia and Western Venezuela. *Palaeogeogr. Palaeoclimatol. Palaeoecol.*, **153**, 239–275.

Villamil, T. & Arango, C. (1998) Integrated stratigraphy of latest Cenomanian and early Turonian Facies of Colombia. In: *Paleogeographic Evolution and Non-Glacial Eustasy, Northern South America* (Ed. by J. Pindell & C. Drake), *SEPM Spec. Publ.* **58**, 129–159.

Watts, A.B. & Ryan, W.B. (1976) Flexure of the lithosphere and continental margin basins. *Tectonophysics*, **36**, 25–44.

Wing, S.L., Herrera, F., Jaramillo, C., Gomez, C., Wilf, P. & Labandeira, C.C. (2009) Late Paleocene fossils from the Cerrejón formation, Colombia, are the earliest record of Neotropical rainforest. *Proc. Natl. Acad. Sci.*, **106**, 18627–18632.

Manuscript received 12 August 2009; Manuscript accepted 15 October 2010.